



## Evidence for high-elevation salar recharge and interbasin groundwater flow in the Western Cordillera of the Peruvian Andes

Odney Alvarez-Campos<sup>1</sup>, Elizabeth J. Olson<sup>1</sup>, Lisa R. Welp<sup>1</sup>, Marty D. Frisbee<sup>1</sup>, Sebastián A. Zuñiga Medina<sup>2</sup>, José Díaz Rodríguez<sup>2</sup>, Wendy R. Roque Quispe<sup>3</sup>, Carol I. Salazar Mamani<sup>3</sup>, Midhwar R. Arenas Carrión<sup>3</sup>, Juan Manuel Jara<sup>3</sup>, Alexander Ccancapa-Cartagena<sup>4,5</sup>, and Chad T. Jafvert<sup>4,6</sup>

<sup>1</sup>Earth, Atmospheric, and Planetary Sciences, Purdue University, West Lafayette, Indiana 47907, USA

<sup>2</sup>Departamento de Geología, Geofísica y Minas, Universidad Nacional de San Agustín de Arequipa, Arequipa, Peru

<sup>3</sup>Departamento de Ingeniería Ambiental, Universidad Nacional de San Agustín de Arequipa, Arequipa, Peru

<sup>4</sup>Lyles School of Civil Engineering, Purdue University, West Lafayette, Indiana 47907, USA

<sup>5</sup>Escuela Profesional de Antropología, Universidad Nacional de San Agustín de Arequipa, Av.

Venezuela S/N, 04000, Arequipa, Peru

<sup>6</sup>Division of Environmental and Ecological Engineering, Purdue University, West Lafayette, Indiana 47907, USA

**Correspondence:** Lisa R. Welp (lwelp@purdue.edu) and Marty D. Frisbee (mdfrisbee@purdue.edu)

Received: 29 May 2021 – Discussion started: 4 June 2021

Revised: 29 October 2021 – Accepted: 9 December 2021 – Published: 31 January 2022

**Abstract.** Improving our understanding of hydrogeological processes on the western flank of the central Andes is critical to communities living in this arid region. Groundwater emerging as springs at low elevations provides water for drinking, agriculture, and baseflow. However, the high-elevation sources of recharge and groundwater flow paths that convey groundwater to lower elevations where the springs emerge remain poorly quantified in the volcanic mountain terrain of southern Peru. In this study, we identified recharge zones and groundwater flow paths supporting springs east of the city of Arequipa and the potential for recharge within the high-elevation closed-basin Lagunas Salinas salar. We used general chemistry and isotopic tracers ( $\delta^{18}\text{O}$ ,  $\delta^2\text{H}$ , and  $^3\text{H}$ ) in springs, surface waters (rivers and the salar), and precipitation (rain and snow) sampled from March 2019 through February 2020 to investigate these processes. We obtained monthly samples from six springs, bimonthly samples from four rivers, and various samples from high-elevation springs during the dry season. The monthly isotopic composition of spring water was invariable seasonally in this study and compared to published values from a decade prior, suggesting that the source of recharge and groundwater flow paths that support spring flow is relatively stable with time. The chemistry of springs in the low-elevations and mid-elevations (2500 to 2900 m a.s.l.) point towards a mix of

recharge from the salar basin (4300 m a.s.l.) and mountain-block recharge (MBR) in or above a queñuales forest ecosystem at  $\sim 4000$  m a.s.l. on the adjacent Pichu Pichu volcano. Springs that clustered along the Río Andamayo, including those at 2900 m a.s.l., had higher chloride concentrations, indicating higher proportions of interbasin groundwater flow from the salar basin likely facilitated by a high degree of faulting along the Río Andamayo valley compared to springs further away from that fault network. A separate groundwater flow path was identified by higher sulfate concentrations (and lower  $\text{Cl}^-/\text{SO}_4^{2-}$  ratios) within the Pichu Pichu volcanic mountain range separating the city from the salar. We conclude that the salar basin is not a hydrologic dead end. Instead, it is a local topographic low where surface runoff during the wet season, groundwater from springs, and subsurface groundwater flow paths from the surrounding mountains converge in the basin, and some mixture of this water supports groundwater flow out of the salar basin via interbasin groundwater flow. In this arid location, high-elevation forests and the closed-basin salar are important sources of recharge supporting low-elevation springs. These features should be carefully managed to prevent impacts on the down-valley water quality and quantity.

## 1 Introduction

Predicted climate change in the tropical Andes includes increases in temperature and evapotranspiration and changes in precipitation patterns (Urrutia and Vuille, 2009; Somers et al., 2019). A  $\sim 10\%$ – $30\%$  reduction in precipitation is projected for the western Andes in the coming century (Minvielle and Garreaud, 2011; Neukom et al., 2015). These changes are projected to have a negative impact on the long-term sustainability of critical groundwater resources in southern Peru (Vuille et al., 2018). High-elevation zones of groundwater recharge in the Andes are extremely sensitive to the interplay between evapotranspiration and precipitation due to climate and anthropogenic land-use change altering vegetative land cover, energy balance, and water balance. Recharge occurring in the mountain block at high elevations is called mountain-block recharge (MBR; see Manning and Solomon, 2003; Wilson and Guan, 2004; Wahi et al., 2008; Ajami et al., 2011; Bresciani et al., 2018). If the amount of precipitation decreases in high-elevation recharge zones, then the amount of effective precipitation (precipitation minus evapotranspiration) potentially available for MBR likewise decreases (Goulden et al., 2012; Goulden and Bales, 2014). In addition, if the land cover changes in the recharge zone (e.g., changes in vegetation type, density, health and/or movement of the treeline), then the MBR will also change. While the effects of MBR reduction may not be immediately felt in the region, they are not inconsequential. Groundwater flow within the mountain block impacts spring flow, headwater streams that originate in the mountain block and subsequently flow across the mountain front, and groundwater wells often located at lower elevations along the mountain front or in adjacent valleys. The importance of MBR on groundwater resources in the Andes and how they might respond to changing precipitation and temperature and melting glaciers is poorly understood (Somers et al., 2018, 2019).

Springs emerging within and down-gradient from the mountain block are important in the high, arid Andes of Peru for a variety of reasons. They provide a source of potable water and can be used for irrigation and recreation, and some have ecological or religious significance (Stensrud, 2019; Sedapar, 2018; Gerencia Regional de Agricultura de Arequipa, 2015). Communities at lower elevations of the western Andes receive very low annual precipitation and rely on surface runoff and groundwater originating from higher elevations (Urrutia and Vuille, 2009). Consequently, identifying groundwater recharge zones and source areas for springs can help us better understand the potential impact of climate change to water resources and better inform water management plans including the protection of perennial springs and their high-elevation recharge zones. This is complicated by the presence of closed-basin salars at high elevations in southern Peru (Juvigné et al., 1997). Some of the runoff that occurs during the wet season is captured by these basins and does not contribute (at least directly) to surface runoff

across the mountain front. Furthermore, these basins are not usually considered a recharge zone (Peña, 2018); however, these salars are local topographic lows and are likely points of groundwater discharge from the surrounding mountains.

There are more than 100 salars in topographic depressions in the high mountainous arid region of the Central Andes (Warren, 2016). These salars occur within a tectonically active region with largely interior (endorheic) drainage from the Andean highland plateaus of Chile, Bolivia, Argentina, and southern Peru. Endorheic basin salars form because the topography of the region favors water accumulation in depressions, and evaporation rates are very high (Warren, 2016). Salars are generally considered closed basins, but not all salars are terminal lakes (Warren, 2016; Risacher et al., 2003). This means that salar brines can infiltrate, be transported elsewhere, and/or mix with meteoric waters (Warren, 2016; Risacher et al., 2003). By using the ratio of the total mass of chloride (assumed to be a conservative tracer and assuming insignificant wind erosion) in the brine lakes to the annual input flux to estimate the tracer's residence time, Risacher et al. (2003) determined that the residence times of  $\text{Cl}^-$  in Chilean brine lakes were short (a few to hundreds of years) in a flow-through steady-state condition. This means that most dissolved salts entering salars in this region are lost by leakage through bottom sediments and reenter the hydrologic system (Risacher et al., 2003), which suggests that salars may play an important role as sources of groundwater recharge despite differences in buoyancies between the brines and fresh-water recharge. In general, the potential for high-elevation closed-basin salars, which are commonly thought to represent the hydrological dead end of surface flow paths, to contribute groundwater recharge to support springs in the central Andes remains uncertain. This begs the following question: are all high-elevation salars simply evaporation pans, or can leakage beneath the salar contribute to groundwater recharge?

Hydrogeological studies have been conducted in salars and groundwaters of Chile to understand groundwater recharge processes, sources of spring flow, the hydrogeologic connectivity of high-elevation mountains and salar basins to the down-valley aquifers, and residence times of groundwaters in these basins (Boutt et al., 2016; Jayne et al., 2016; Scheihing et al., 2018; Herrera et al., 2016; Fritz et al., 1981). Groundwater stable isotopes depleted in deuterium ( $^2\text{H}$ ) and oxygen-18 ( $^{18}\text{O}$ ) suggest that the main source of aquifer recharge is precipitation at high elevations ( $\sim 4000$  m a.s.l.) of the Altiplano and Andean mountain ridge (Jayne et al., 2016; Scheihing et al., 2017). Early stable isotope research proposed that groundwater recharge to the Pampa del Tamarugal ( $\sim 1000$  m a.s.l.), which is the most economically important aquifer in the Atacama Desert, occurs in the nearby Pre-cordillera, Altos de Pica ( $\sim 3500$  m a.s.l.; Fritz et al., 1981). Subsequent studies pointed to recharge further inland at the Salar de Huasco basin ( $\sim 3700$  m a.s.l.) through deep fissures that connect the salt-crust salar to springs in the town of

Pica and the Pampa de Tamarugal (Magaritz et al., 1989, 1990). However, recent research rejected the possible influence of the high-elevation Salar de Huasco to groundwater recharge of lower elevation springs based on isotopic characterization (Uribe et al., 2015) and geothermometer inference (Scheihing et al., 2017). Nearby, Herrera et al. (2016) suggest that there may be a small amount of recharge from Laguna Tuyajto (4010 m a.s.l.) in Chile to the underlying Salar de Aguas Calientes-III basin (3939 m a.s.l.). Furthermore, they state that, despite differences in buoyancy between saline brines and fresh groundwater, some proportion of the saline water from Laguna Tuyajto likely mixes and becomes incorporated with regional groundwater flow. Tritium ( $^3\text{H}$ ) offers insight into these mixing processes and can provide valuable information on residence times of groundwater that stable isotopes typically cannot. For example, Moran et al. (2019) used tritium ( $^3\text{H}$ ) to age-date waters across the Salar de Atacama in Chile from the surrounding mountains to the basin lagoons and found evidence of  $^3\text{H}$ -dead groundwater inferred to be older than 60 years. Their data indicate that groundwater discharge to the Salar de Atacama is interbasin flow of pre-bomb recharge from other internally drained basins at higher elevations.

The salars and mountain-groundwater systems of Peru have received much less attention compared to Chile. Few hydrogeological studies have quantified groundwater recharge processes in southern Peru. Arequipa (2300 m a.s.l.) is Peru's second largest city (with a population exceeding 1 million), and it is situated near a high-elevation (4300 m a.s.l.) closed-basin salar, Laguna Salinas. Local research conducted on the source of springs east of the city of Arequipa by the Peruvian Agency INGEMMET ("Instituto Geológico, Minero y Metalúrgico") indicates that the zone of groundwater recharge is precipitation on a nearby high-elevation volcano called Pichu Pichu (Peña, 2018). However, the potential influence of the Lagunas Salinas basin and the salar itself as a recharge source for the lower elevation springs has not been thoroughly investigated. Due to the importance of groundwater in southern Peru, it is essential to study the hydrogeological behavior of the basins throughout the region. The objectives of this study are (1) to identify sources of recharge and (2) to quantify groundwater flow paths supporting springs near the city of Arequipa using natural geochemical and isotopic tracers measured in springs, surface waters (rivers and salar), and precipitation (rain and snow). We assessed the contribution of high-elevation precipitation or salar recharge using a combination of stable isotopes ( $\delta^{18}\text{O}$  and  $\delta^2\text{H}$ ) and geochemical tracers. Tritium ( $^3\text{H}$ ) was used as a reconnaissance tool on a subset of springs to provide insight into the ranges of residence times for these springs. Specifically, we address the following question: is the Laguna Salinas a source of recharge for the deeper groundwater system that supports low-elevation springs in the Arequipa region?

## 2 Study area

Our study is in the Central Andes of southwestern Peru in the department of Arequipa between the Andean Western Cordillera and the coastal belt at  $16^{\circ}20'$  S latitude and  $71^{\circ}30'$  W longitude (Fig. 1). In this section we provide context for the study and a description of the potential geologic controls on the hydrology of the region.

### 2.1 Water uses

The Río Chili, which flows through the city, and La Bedoya spring to the east are the two main sources of drinking water for the metropolitan area of Arequipa (Sedapar, 2018). Commercial crop production and self-consumption rely on these water resources in addition to large-scale water diversion projects from the neighbouring Majes watershed (MINCETUR, 2017; Gerencia Regional de Agricultura de Arequipa, 2015). Water-intensive mining activities also occur throughout Arequipa, including the Cerro Verde mine just south of the city (MINCETUR, 2017). According to census data from 2007 to 2017, population growth in arid coastal areas of Peru increased 1.3 % annually, and the capital city population increased 2.3 % annually (from 806 782 to 1 008 290 people from 2007 to 2017) (INEI, 2018). Continued population growth and a growing agricultural sector stress water resources in southern Peru.

### 2.2 Climate

The western central Andes has experienced an arid to semi-arid climate since the modern Andes were uplifted in the middle Miocene, forming a barrier to easterly winds (Warren, 2016). In the early to middle Pleistocene, several glaciations occurred in this region; however, most Andean glaciers have receded since the mid-19th century (Seltzer, 1990; Ehlers et al., 2011). Today, the western part of the Central Andes is characterized by a strong annual cycle of precipitation, consisting of a very dry winter (June to August) and a wet summer monsoon season (November to April) bringing precipitation from the Amazon with large interannual variability (Garréaud, 2009; Urrutia and Vuille, 2009; Imfeld et al., 2021). The Pichu Pichu volcano commonly accumulates snow during the summer wet season. Average annual precipitation is higher (400–600 mm at elevations above 4000 m a.s.l.) compared with lower elevations in the department of Arequipa ( $\sim 100$  mm) (Moraes et al., 2019). Annual average temperatures are cooler at higher elevations and warmer at lower elevations near the coast, except for near large rivers such as the Río Majes and Río Tambo (Moraes et al., 2019). Figures S1 and S2 in the Supplement show the monthly mean precipitation and temperature climatology at three elevations within our study region.

There are two meteorological stations operated by the Peruvian Servicio Nacional del Meteorología e Hidrología del

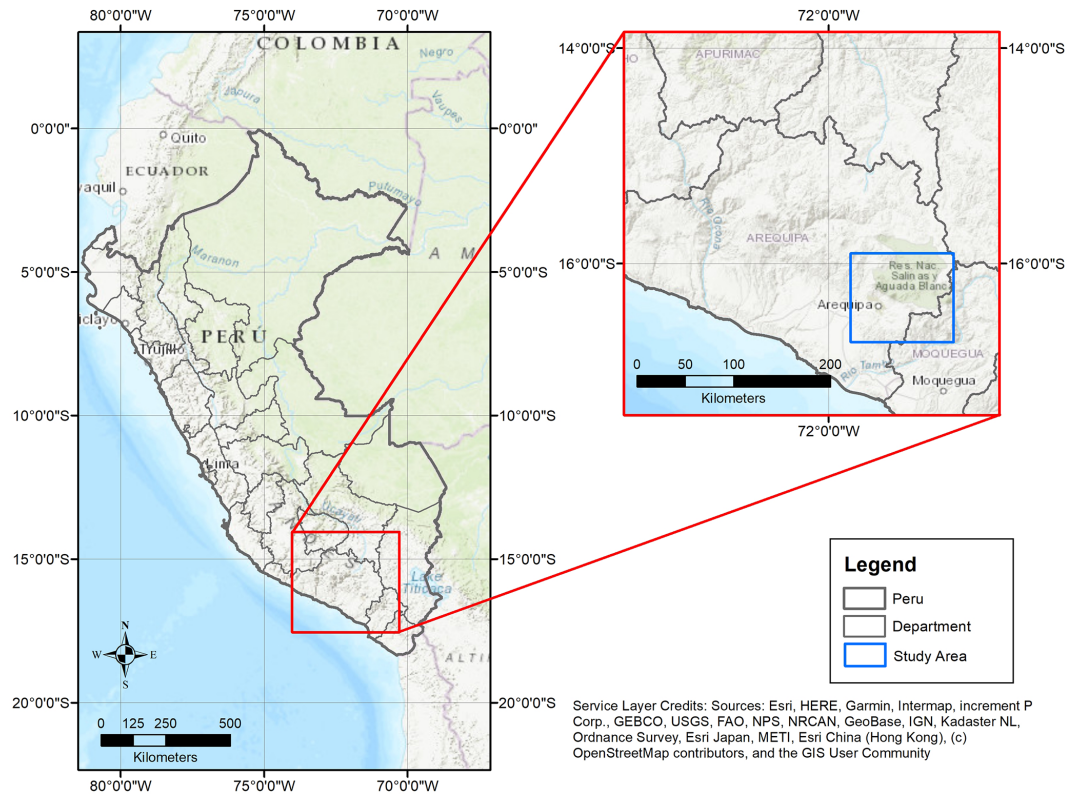


**Figure 1.** Map of the Arequipa department in southern Peru, the Quilca–Vitor–Chili River basin, and our study area in the northeastern part of this basin.

Perú (SENAMHI) in our study watershed, located in the districts of Chiguata and Salinas Huito (near Laguna Salinas) (Senamhi, 2020). Annual 2018 precipitation was 140 mm for Chiguata (2902 m a.s.l.) and 350 mm for Salinas Huito (4349 m a.s.l.). The 2018 annual maximum temperature for Chiguata and Salinas Huito was 20.3 and 12.7 °C, respectively, while minimum temperatures were 5.9 and −4.7 °C. Data for 2019 had many gaps and quality control issues at Salinas Huito, so they are not reported here.

### 2.3 Geologic description

Our study focuses on the Chili watershed, which can be divided in three main geomorphologic landforms largely shaped by tectonic and volcanic processes: (1) the Arequipa depression; (2) the Western Cordillera, which comprises the Grupo Barroso and cluster of volcanoes; and (3) the highland hills and depressions surrounding Laguna Salinas (Peña, 2018; Thouret et al., 2001).

The complex geology of the region includes rock units of high and low permeability and faulting that influence groundwater flow paths. Low-permeability basement rock of the Arequipa massif (Jenks, 1948; Peña, 2018) limits hydrologic conductivity at depth and creates a barrier to groundwater flow (Guevara, 1965) and possibly deep circulation. This Pre-Cambrian feldspathic Charcani gneiss is exposed in

small outcrops along river channels of the districts of Mollebaya and Yarabamba. Thick volcanic deposits and carbonate formations associated with extensional processes during back-arc formation of the Arequipa–Tarapacá basin overlie the basement Charcani gneiss (Sempere et al., 2002; Vicente, 2006). Thick sediments of the Mesozoic Socosani formation with sequences of limestones interbedded with black shales and sandstone are ca. 80 m thick in Arequipa (Jenks, 1948). Detrital clastic sediments of the Grupo Yura contain sequences of sandstone interbedded with thin layers of shales and limonites. The Grupo Yura is overlain by younger volcanic deposits from the late Miocene to Pleistocene from the Grupo Barroso, which is characterized by porphyritic andesite lavas from volcanoes Pichu Pichu and Misti. Local confined and unconfined aquifers have previously been identified within permeable units interbedded between baked contacts within the Grupo Barroso (Peña, 2018). Fluvio-glacial fill deposits on the slopes of Pichu Pichu volcano lay beneath more recent pyroclastic and clastic materials (Thouret et al., 2001). A landslide of pyroclastic deposits ca. 400 m thick outcrop along the Río Andamayo gorge with a pseudotachylyte basal contact with the underlying ignimbrite may limit deep circulation in the Charcato area (Legros et al., 2000). Springs in our Chiguata study site lay above paleolake deposits comprised of high-

permeability sandstones and thin units of low-permeability stratified diatomite and clay (García Fernández Baca et al., 2016). Finally, alluvial and fluvial deposits consisting of mainly gravel, sand, silt, and poorly consolidated conglomerates are distributed in the banks of the Río Chili, Río Andamayo, and Río Yarabamba.

Faults are common throughout the study area (Fig. 2). Some of the faults are associated with volcanic activity (ring-fracture faults and normal faults), and others are associated with strike-slip plate motion. These faults are likely hydrogeologically important because the fractures associated with the faults can either enhance groundwater flow or act as barriers directing groundwater to the surface. The Western Cordillera volcanic complexes (Misti and Pichu Pichu) are aligned along a strike-slip fault that trends from NW to SE (Mering et al., 1996; Thouret et al., 2001). While many faults have been mapped in this region (Fig. 2; Thouret et al., 2001; Lebti et al., 2006; Bernard et al., 2019), the normal faults (NW to SE direction) in the district of Chiguata are most relevant to our study (Benavente et al., 2017; Thouret et al., 2001). The Río Andamayo flows along a fault separating the older Pichu Pichu mountain block from the uplift associated with Misti (Fig. 2).

In the highlands, the Laguna Salinas closed-basin salar likely formed during the creation of the late Miocene to early Quaternary volcanic range, which includes the Pichu Pichu, Misti, Ubinas, and Chachani volcanoes (Lebti et al., 2006); and following an eruption of the Pichu Pichu volcano in 6.7 Ma (Kaneoka and Guevara, 1984; Jean-Claude Thouret, personal communication, 2020). The salar covers  $\sim 142 \text{ km}^2$  (Garrett, 1998) and floods to an average depth of 50 cm during the rainy season from December to March and then nearly completely dries during the long dry season. Springs from higher elevations in the surrounding mountains contribute water to the salar basin, but there is no surface outflow draining it. Water loss is entirely evaporation and potentially groundwater recharge. Economically important evaporite minerals form in the salar during the dry season. These minerals, ulexite, halite, Glauber salt, and thenardite, are found at the crust of the salar and with depth in the lacustrine deposits (Muessig, 1958; Garrett, 1998). The lacustrine deposits consist of layers of halite and thenardite ( $\text{Na}_2\text{SO}_4$ ) at the surface (5–15 cm), followed by a thin white volcanic ash layer ( $< 15 \text{ cm}$ ), various mud layers containing ulexite ( $\text{NaCaB}_5\text{O}_9 \cdot 8\text{H}_2\text{O}$ ;  $\sim 1.5\text{--}1.8 \text{ m}$ ), and the main ulexite bed occurs between 0.25 to 1.3 m in the lacustrine sediments. Inyoite ( $\text{Ca}_2\text{B}_6\text{O}_{11} \cdot 13\text{H}_2\text{O}$ ) is also present beneath the ulexite bed along the eastern side of the salar near the Tusca Hot Spring ( $< 15 \text{ cm}$ ; Muessig, 1958; Garrett, 1998).

## 2.4 Watershed description and sampling locations

The Río Chili watershed drainage is part of the Quilca–Vitor–Chili River basin, extending from the Andean Altiplano to sea level at the Pacific coast. Our research was conducted

in the districts of Characato ( $\sim 2500 \text{ m a.s.l.}$ ) and Chiguata ( $\sim 3000\text{--}3500 \text{ m a.s.l.}$ ) and the high-elevation closed-basin salar, Laguna Salinas ( $\sim 4300 \text{ m a.s.l.}$ ), 80 km east of the city of Arequipa (Fig. 2). The dormant Pichu Pichu volcano ( $5510 \text{ m a.s.l.}$ ) forms a seasonally snow-covered ridge between the city of Arequipa and Laguna Salinas. The active Ubinas volcano ( $5672 \text{ m a.s.l.}$ ) is located northeast from Laguna Salinas in a Quaternary volcanic range. Precipitation that falls on Ubinas can drain toward Laguna Salinas or the Río Tambo. The salar is bordered to the north by the Pukasaya mountains. We sampled springs emerging within the Río Andamayo watershed draining the southwestern slope of the Pichu Pichu volcano and with a headcut approaching the Laguna Salinas. Additional samples in the upper drainage were obtained from the queñuales forest, named after the tree species (*Polylepis* sp.) endemic to the high Andean forest ecosystems above  $3500 \text{ m a.s.l.}$  (Camel et al., 2019). Several smaller rivers, the Mollebaya, Socabaya, and Characato, also join the Andamayo, although they head at lower elevations. The Río Andamayo joins the Río Chili in the city of Arequipa, forming the Río Vitor, which flows into the Río Quilca and eventually the Pacific Ocean.

## 3 Methods

### 3.1 Water sampling

Table 1 lists coordinates, elevation, names, and IDs of water samples collected in this study. We sampled a total of six low-elevation springs once a month from March 2019 to February 2020. Four springs (SAN, YUM, ANA, and OJO) were obtained in the district of Characato ( $\sim 2500 \text{ m a.s.l.}$ ), and two springs (BED and BAD) were sampled in the district of Chiguata ( $\sim 2900 \text{ m a.s.l.}$ ) (Fig. 2, Table 1). We collected river water samples once every 2 months at two locations ( $2783 \text{ m a.s.l.}$  elevation at Chiguata and  $2419 \text{ m a.s.l.}$  elevation at Characato) on the Río Andamayo (ATA and AND respectively), which drains from the highlands to the city of Arequipa, and at three smaller rivers, Río Socabaya (SOC), Río Mollebaya (MOL and MOY), and Río Characato (RCH). The river flow in the Río Mollebaya dried up at the initial sampling point (MOL) in the dry season, so the collection location was moved upstream (MOL) 115 m in elevation to continue collecting water. We sampled Laguna Salinas surface water at the end of the rainy season (April 2019) and during the dry season (October 2019). We sampled six smaller high-elevation springs (TSA, INK, HUM, UBI, MOQ, and PAT) once in October 2019 near Laguna Salinas above  $4330\text{--}4429 \text{ m a.s.l.}$  The spring INK emerges at the salar, and this spring is only accessible during the dry season. During the wet season, the INK spring is covered by standing water. The spring TSA emerges near the town of Salinas Huito, while HUM, UBI, MOQ, and PAT emerge from the lower slopes of the Tacune mountain ( $5500 \text{ m a.s.l.}$ ), south of the

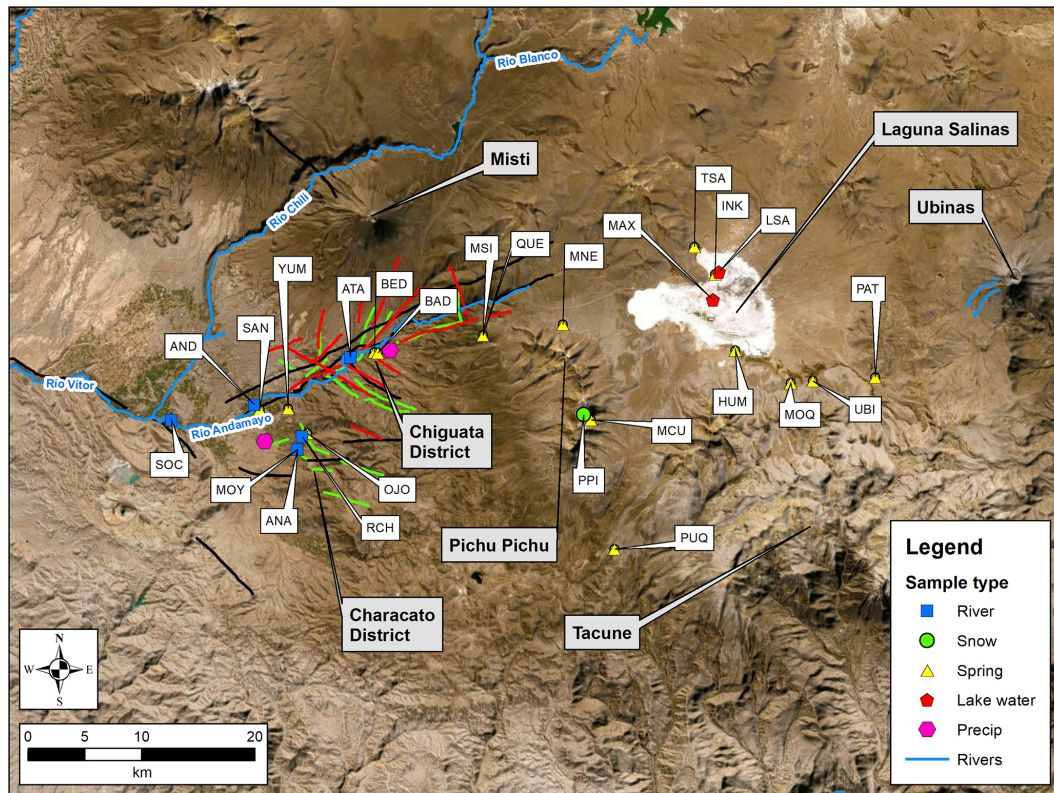


**Figure 2.** Map of the study area, sampling locations, and faults identified. The different types of water are indicated by different symbols in the legend. Green lines are faults identified in Bernard et al. (2019); black lines are faults identified in Lebti et al. (2006); and red lines are faults identified in Thouret et al. (2001). The Río Andamayo is fault-bounded (black lines running parallel to the river). The La Bedoya (BED) and El Badén (BAD) springs are located in the Chiguata District. The springs Sabandia (SAN), Yumina (YUM), Ojo de Characato (OJO), and Santa Ana (ANA) are located in the Characato District. Blue lines are rivers. (credit: Emily E. Frisbee).

salar. We sampled snow from the Pichu Pichu volcano (PPI; 5106 m a.s.l.) once in April and two high-elevation springs in the area in May 2019 (MNE and MCU, 4657–4888 m a.s.l.). Snow was collected at the surface and at  $\sim 10$  cm depth placed in Ziploc bags and allowed to melt at room temperature before being transferred to 1 L bottles. We also sampled three springs (MSI, PUQ, and QUE) in the high-elevation queñuales forest (3770 – 4052 m a.s.l.) in May and October 2019. Pluviometers installed in Characato (2300 m a.s.l.) near the La Pampilla SENAHEMI station and in Chiguata (2969 m a.s.l.) as part of a complementary research effort were used to collect daily rainwater during the wet season from January to March (Welp et al., 2022). The rest of the year there is almost no precipitation (Fig. S1). Rain gauges were emptied each morning to minimize evaporation.

Spring, river, and salar water samples were collected using a collection tube below the surface of the river or the spring emergence connected to a hand pump and filtered using a  $0.45 \mu\text{m}$  membrane into 25 mL (with poly-seal caps) and 250 mL plastic bottles for stable isotope and general chemistry analysis respectively. If the spring emergence was not accessible, the closest possible pool of flowing water was

sampled. Additional 1 L samples for tritium ( $^3\text{H}$ ) analyses were collected at four sites (INK, UBI, OJO, and BED) in September 2019, Pichu Pichu snow (PPI) from May 2019, and Arequipa precipitation (MID) from February 2020. All plastic bottles were tightly closed and sealed with electrical tape to prevent water leakage and reduce evaporation. Water temperature ( $^{\circ}\text{C}$ ) and pH were measured in situ at all sites using a handheld Oakton meter (AO-35423-01). Electrical conductivity (EC) was measured in the field using a YSI Professional Plus (Quatro) multi-parameter probe. The YSI probe calculates (1) specific conductivity ( $\text{SpC}$ ,  $\mu\text{S cm}^{-1}$ ) from  $\text{SpC} = \text{EC} \cdot 1.91$ , where 1.91 is the temperature coefficient at  $25^{\circ}\text{C}$ ; and (2) total dissolved solids (TDS, ppm) from  $\text{TDS} = \text{EC} \cdot 0.65$  (Table S1 in the Supplement). Both instruments were calibrated daily and recalibrated at different altitudes.

### 3.2 Isotopic analysis

Stable isotopes of water ( $^2\text{H}$  and  $^{18}\text{O}$ ) were measured at Purdue University on a Liquid Water Isotope Analyzer (Los Gatos Research, San Jose, California, USA, model T-LWIA-45-EP). The first 4 of 10 total injections were excluded due

**Table 1.** Location, sample ID, elevation, and months sampled of springs, snow, and surface waters. These sites are mapped in Fig. 2.

Sample group/location	Sample ID (name)	Sampling dates (mm/yyyy)	Elevation (m a.s.l.)	Lat.	Long.
Characato springs	SAN (Sabandia)	Once a month from 03/2019 to 02/2020	2431	-16.4497	-71.4955
	YUM (Yumina)		2590	-16.4488	-71.4730
	ANA (Santa Ana)		2518	-16.4812	-71.4655
	OJO (Ojo de Characato)*		2595	-16.4687	-71.4575
Chiguata springs	BED (La Bedoya)*		2899	-16.4042	-71.4044
	BAD (El Baden)		2900	-16.4046	-71.4018
Laguna Salinas salar springs	TSA (Tambo de Sal)	10/2019	4332	-16.3204	-71.1507
	HUM		4330	-16.4029	-71.1182
	INK*		4324	-16.3423	-71.1342
	MOQ		4346	-16.4286	-71.0742
	PAT		4429	-16.4241	-71.0072
	UBI*		4347	-16.4269	-71.0567
Pichu Pichu springs	MNE	05/2019	4657	-16.3823	-71.2549
	MCU		4888	-16.4577	-71.2326
Queñuales springs	MSI	05/2019	4052	-16.3908	-71.3183
	PUQ	10/2019	3770	-16.5605	-71.2141
	QUE	10/2019	4011	-16.3908	-71.3184
Laguna Salinas salar	LSA	04/2019 and 10/2019	4317	-16.3405	-71.1313
Surface water	MAX	10/2019	4322	-16.3624	-71.1361
Characato rivers	SOC (Socabaya)	03, 06, 09/2019 and 02/2020	2206	-16.4581	-71.5656
	AND (Andamayo in Characato District)		2419	-16.446	-71.4997
	MOL (Mollebaya during wet season)	03/2019	2401	-16.4893	-71.5020
	MOY (Mollebaya starting the dry season)	06, 09, 12/2019 and 02/2020	2516	-16.4815	-71.4656
	RCH (Characato)	03, 04, 06, 09, 12/2019 and 02/2020	2541	-16.4713	-71.4618
Chiguata River	ATA (Andamayo in Chiguata District)	03, 04, 06, 09, 12/2019 and 02/2020	2783	-16.4082	-71.4234
Precipitation	PPI* (Pichu Pichu snow)	05/2019	5106	-16.4537	-71.2385
	PCP-Chiguata (rain)	Daily in 2020 wet season	2969	-16.4029	-71.3919
	PCP-Characato (rain)	Daily in 2019 and 2020 wet season	2300	-16.4750	-71.4916
	MID* (Arequipa rain)	Feb 2020	2355	-16.4068	-71.5241

\* Indicates this site was analyzed for  $^3\text{H}$ . Note: PCP refers to precipitation.

to memory effects (Penna et al., 2012), and the last six injections were averaged for the reported value. Data are reported relative to the international VSMOW-SLAP standard scale (Vienna Standard Mean Ocean Water-Standard Light Antarctic Precipitation), with an analytical error of  $< 0.2\text{‰}$  and  $< 1.0\text{‰}$  for  $\delta^{18}\text{O}$  and  $\delta^2\text{H}$ , respectively.

Tritium ( $^3\text{H}$ ) was analyzed to identify the mixing relationships, sources of recharge, and the presence/absence of modern recharge. The atmospheric  $^3\text{H}$  breakthrough associated with nuclear weapons testing in the 1950s and 1960s

observed in South America and the Southern Hemisphere was not similar to that observed in North America and the Northern Hemisphere. For example, the tritium breakthrough peaked at approximately 60 TU in Cuiabá, Brazil, in 1965, and many equatorial monitoring stations measured breakthroughs less than 40 TU (Albero and Panarello, 1981). In comparison, the atmospheric breakthrough was much higher in the Northern Hemisphere; the tritium breakthrough in Miami, FL, USA, peaked at 384 TU in 1964 while the peak was over 3800 TU in Chicago, IL, USA, in 1964. Thus, it

is not unusual to find tritium-dead groundwater in the Southern Hemisphere since the  $^3\text{H}$  in recharge occurring during the bomb-pulse era has largely decayed back to pre-bomb levels. Regardless,  $^3\text{H}$  measurements in springs and groundwater from salars may still be useful as a reconnaissance tool for future age dating, especially if modern samples of precipitation and other appropriate endmembers are characterized for comparison.

Samples of 1 L were collected for  $^3\text{H}$  in the field, stored in high-density polyethylene bottles with leak-free caps and were not exposed to indoor air. Samples PPI, OJO, BED, INK, and UBI, as well as a one-time 1 L sample of rain within the city of Arequipa during February 2020, were analyzed for  $^3\text{H}$  at the University of Miami, Tritium Lab. Water samples were distilled, enriched via an electrolyzed water bath for 10 to 14 d, reduced over hot magnesium metal, and transferred to the counter for 6 to 20 h. Backgrounds are set by comparison to tritium-dead petroleum and deep Florida Aquifer waters. Efficiency is determined by preparation of the NIST SRM no. 4926 standard water (Östlund et al., 1987). The reported accuracy and precision for ultralow-activity electrolytic enrichment through volume reduction is 0.1 TU.

### 3.3 Chemical analysis

Cation ( $\text{Ca}^{2+}$ ,  $\text{Mg}^{2+}$ ,  $\text{Na}^+$ , and  $\text{K}^+$ ) and anion ( $\text{Cl}^-$ ,  $\text{Br}^-$ ,  $\text{SO}_4^{2-}$ , and  $\text{HCO}_3^-$ ) analyses were conducted by the New Mexico Bureau of Geology & Mineral Resources. Cations were measured by inductively coupled plasma optical emission spectrometry (ICP-OES, PerkinElmer Optima 5300 DV) following EPA Method 200.7 (USEPA, 1994). Anions were measured by ion chromatography (IC-Dionex ICS-5000) following EPA Method 300.0 (USEPA, 1993). Precision for major ions varied by ion but was  $< 6 \text{ mg L}^{-1}$  for everything reported here. Additional precision details can be found in Table S1. Boron and Lithium concentrations were determined using ICP-OES at Purdue University (iCAP 7400, Thermo Scientific, China) with dual plasma view, equipped with Qtegra ISDS software. Concentration standards for both ranged from 2 to 2000 ppb and had correlation coefficients of 0.9959 for B and 0.9948 for Li. The limits of detection for B and Li were 1.1 and 0.1 ppb, and the limits of quantification were 3.6 and 0.2 ppb, respectively. The accuracies for both elements were above 90%. Values above 2000 ppb were reported as above the maximum calibration range.

## 4 Results

### 4.1 Isotopic composition of precipitation, surface springs, and salar water

The local meteoric water line (LMWL) calculated from daily rain collections in 2019–2020 was  $\delta^2\text{H} = 8.0\delta^{18}\text{O} + 10.9\text{‰}$ . The monthly isotopic composition of Characato and Chiguata springs was largely invariable over time (Ta-

ble S1). The monthly stable isotopic composition of the springs in the district of Characato ranged from  $-8.7\text{‰}$  to  $-10.1\text{‰}$  for  $\delta^{18}\text{O}$  and  $-58\text{‰}$  to  $-68\text{‰}$  for  $\delta^2\text{H}$  (Fig. 3), with mean values reported in Table 2. Springs in the district of Chiguata have more depleted isotopic compositions with monthly values ranging from  $11.6\text{‰}$  to  $-12.9\text{‰}$  for  $\delta^{18}\text{O}$  and  $-85\text{‰}$  to  $-97\text{‰}$  for  $\delta^2\text{H}$  (Fig. 3 and Table S1), with mean values reported in Table 2. Snow from the Pichu Pichu volcano and springs around Laguna Salinas area are even more depleted ( $-14.1\text{‰}$  to  $-16.7\text{‰}$  for  $\delta^{18}\text{O}$  and  $-109\text{‰}$  to  $-126\text{‰}$  for  $\delta^2\text{H}$ ) (Fig. 3 and Table S1). Spring samples collected at the queñuales forest zone have an isotopic composition similar to springs in the Characato District and also the weighted average of rain sampled in Characato in 2019 ( $\delta^{18}\text{O} = -9.5\text{‰} \pm 0.7\text{‰}$ ,  $\delta^2\text{H} = -66\text{‰} \pm 5\text{‰}$ ) (Fig. 3). However, the weighted average rain sampled in 2020 in Characato ( $\delta^{18}\text{O} = -5.7\text{‰} \pm 0.2\text{‰}$ ,  $\delta^2\text{H} = -32\text{‰} \pm 1\text{‰}$ ) and Chiguata ( $\delta^{18}\text{O} = -6.3\text{‰} \pm 0.3\text{‰}$ ,  $\delta^2\text{H} = -38\text{‰} \pm 2\text{‰}$ ) was more enriched, showing that interannual variability in precipitation isotope values can be very large (Table S1). Note that high-elevation precipitation ( $> 3000 \text{ m a.s.l.}$ ) other than Pichu Pichu snow (PPI) was not sampled in this study. Samples from Laguna Salinas surface water (LSA) obtained in the dry season (October 2019) had a highly enriched isotopic composition, while LSA sampled during the wet season (April 2019) had an isotopic composition of  $-16.3\text{‰}$   $\delta^{18}\text{O}$  and  $-122\text{‰}$   $\delta^2\text{H}$ , similar to springs in that area (Fig. 3).

The measured  $^3\text{H}$  activities of modern rainfall from the city of Arequipa and in snow from Pichu Pichu summit were 1.4 and 2.2 TU, respectively. In contrast, the tritium activities of the springs INK and UBI in the Lagunas Salinas basin as well as OJO in Characato and BED in Chiguata were considered  $^3\text{H}$ -dead since lab reported values were at or below the detection limit of 0.1 TU.

In contrast to nearly isotopically constant spring waters, most rivers were more variable (Fig. 4). The exception is the Río Characato (RCH), which only varied by  $1\text{‰}$  in  $\delta^2\text{H}$  during our sampling dates. The Río Socabaya (SOC) and the Río Andamayo sampled at Chiguata (ATA) showed more depleted isotopic values in February 2020. The isotopic composition of the Río Mollebaya (MOL and MOY) was more enriched than most rivers except the Río Characato and also showed slightly more enriched isotopic composition during June and September compared to other months. The isotopic values of the Río Andamayo sampling site at Chiguata in the dry season are comparable to the composition of springs sampled in Chiguata (BED and BAD). Likewise, the isotopic composition of samples from the Río Mollebaya (MOL and MOY) and Río Characato (RCH) were similar to the average spring values sampled in Characato. These similarities suggest that groundwater discharge contributed to river flow in these areas, especially during the dry season.

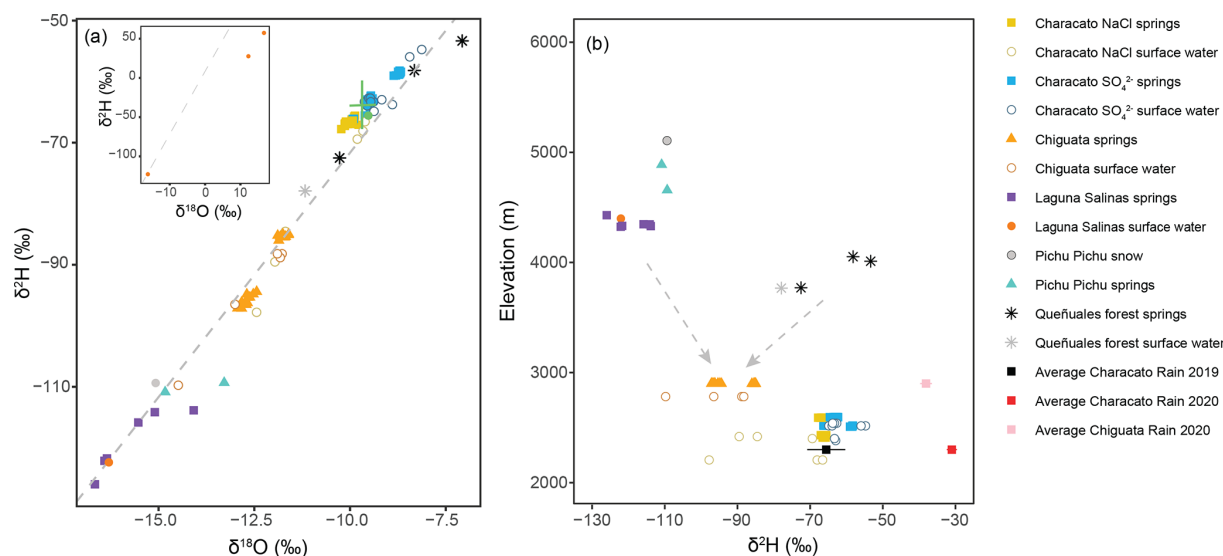


**Figure 3.** (a) Isotopic composition of springs, rivers, and precipitation sampled in our study area. The LMWL (dashed grey line) estimated for this region was  $\delta^2\text{H} = 8.0\delta^{18}\text{O} + 10.9\text{‰}$ . The inset is an adjusted scale to show isotopically enriched dry-season Laguna Salinas surface water (LSA:  $\delta^{18}\text{O} = 12.3$ ,  $\delta^2\text{H} = 28$  and MAX:  $\delta^{18}\text{O} = 16.7$ ,  $\delta^2\text{H} = 57$ ) and 2020 amount-weighted average rain values. (b) Deuterium composition with respect to elevation of springs, rivers, Laguna Salinas wet-season surface water, and precipitation. The isotopic composition of dry-season Laguna Salinas surface water has been omitted. Amount-weighted averages of rain are shown with amount-weighted standard deviation error bars and do not show the full range of daily maximum and minimum values. Surface waters in open symbols with the exception of Lagunas Salinas surface waters which are closed for emphasis. Arrows indicate hypothesized mixing lines between high-elevation sources of recharge. Sample classification (NaCl and  $\text{SO}_4^{2-}$ ) based on chemistry data presented in Sect. 4.2.

**Table 2.** Average isotopic composition for springs sampled from March 2019 to February 2020 and comparison with isotope values of three springs sampled in 2009 by Sulca et al. (2010). Parentheses are standard deviations of all measurements at that site. Discharge from Díaz Rodríguez et al. (1978) compared with measurements in 2016 from Peña Laureano (2018).

Spring name	This study		Sulca et al. (2010)		Peña Laureano (2018)	Díaz Rodríguez et al. (1978)
	March 2019 to Feb 2020		Sampled Nov 2009		Sampled 2016	Sampled 1977
	$\delta^{18}\text{O}$ (‰)	$\delta^2\text{H}$ (‰)	$\delta^{18}\text{O}$ (‰)	$\delta^2\text{H}$ (‰)	Discharge ( $\text{L s}^{-1}$ )	Discharge ( $\text{L s}^{-1}$ )
<b>Characato springs (~ 2500 m)</b>						
Yumina	-10.1 ( $\pm 0.1$ )	-67 ( $\pm 0.4$ )	-10.2	-66	215	255
Sabandía	-9.9 ( $\pm 0.1$ )	-66 ( $\pm 0.4$ )				
Santa Ana	-9.1 ( $\pm 0.6$ )	-61 ( $\pm 3.6$ )				
Ojo de Characato	-9.5 ( $\pm 0.1$ )	-63 ( $\pm 0.6$ )	-9.7	-63	206	216
<b>Chiguata springs (~ 2900 m)</b>						
La Bedoya	-11.7 ( $\pm 0.1$ )	-85 ( $\pm 0.3$ )	-11.8	-85	114	206
El Baden	-12.7 ( $\pm 0.2$ )	-96 ( $\pm 1.0$ )				

## 4.2 Hydrochemical facies and processes

Most chemistry of springs in our study region falls on a mixing line between sodium chloride (NaCl) and calcium sulfate ( $\text{CaSO}_4$ ) water types (Fig. 5). NaCl type waters include Laguna Salinas surface water, three springs near Laguna Salinas (UBI, MOQ, and INK), and springs in the district of Chiguata (BED and BAD). Pichu Pichu snow, one Pichu Pichu spring (MCU) and two Characato springs (OJO and ANA) plot to-

wards the  $\text{CaSO}_4$  quadrant, while the Characato springs that are geographically closer to the Río Andamayo (SAN and YUM) plot in the middle of this inferred mixing line. Since two springs in Characato had greater NaCl percentage (SAN and YUM) than the other two springs (OJO and ANA), we classified samples from Characato into two groups: NaCl and  $\text{SO}_4^{2-}$  springs.

Gibbs diagrams are commonly used to identify relative controls of three processes on water chemistry: precipita-

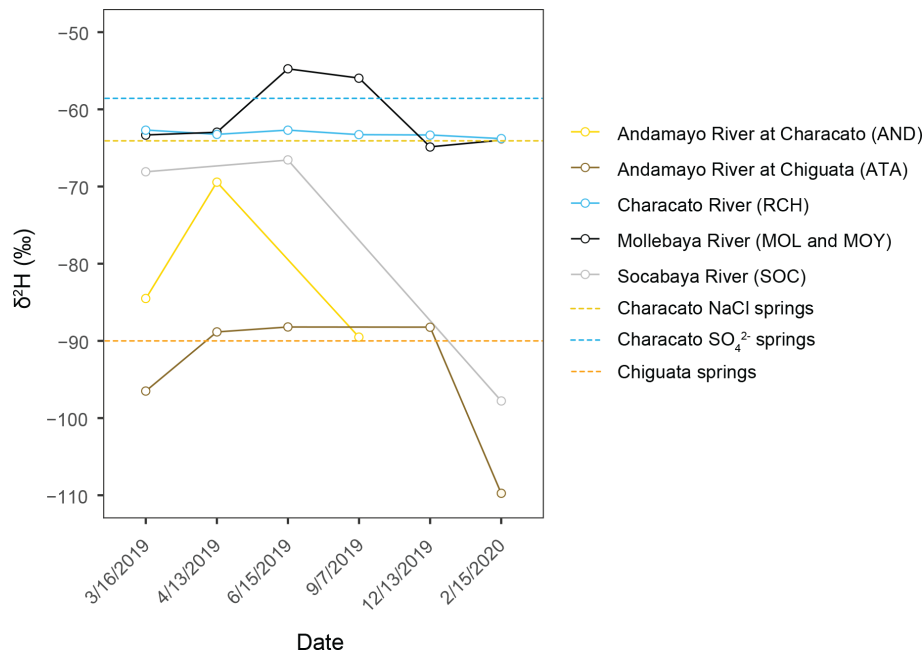


**Figure 4.** Deuterium composition time series of rivers in the Characato and Chiguata districts show isotopic compositions similar to nearby springs, indicating strong groundwater influence on surface waters. MOL and MOY refer to the Río Mollebaya during the wet and dry seasons, respectively. Dashed lines indicate average deuterium compositions of low-elevation springs during the same sampling period. Characato NaCl springs' minimum and maximum are  $-67.8‰$  and  $-65.6‰$ ; Characato sulfate springs' minimum and maximum are  $-66.4‰$  and  $-58.2‰$ ; and Chiguata springs' minimum and maximum are  $-97.2‰$  and  $-85‰$ .

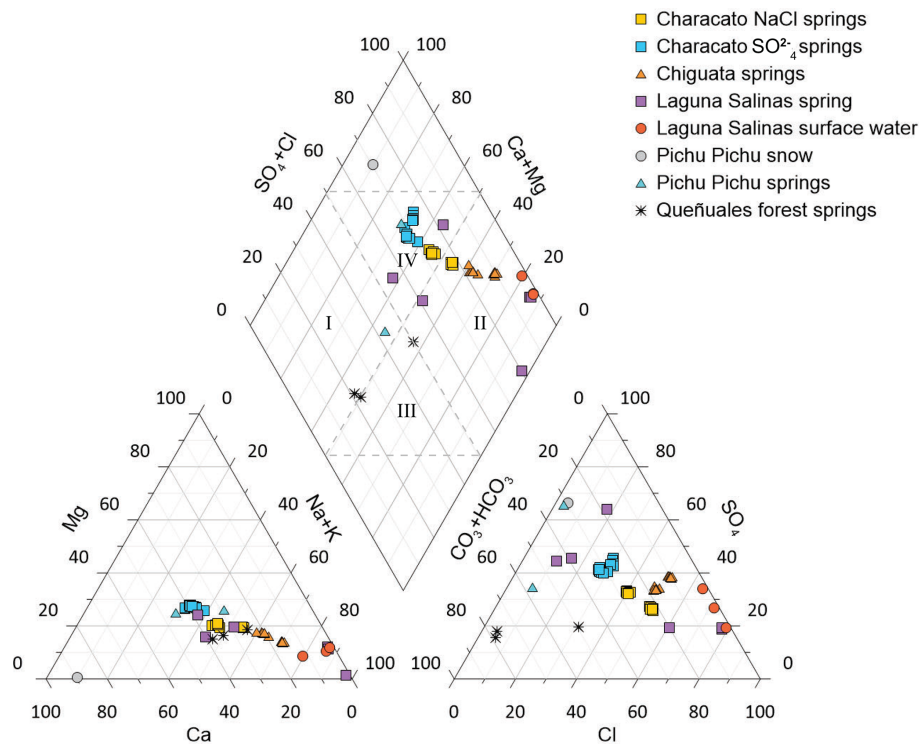


**Figure 5.** Piper diagram of all groundwater samples, Lagunas Salinas surface water, and snow sample in this study. Quadrant I represents calcium-bicarbonate waters, quadrant II represents sodium chloride waters, quadrant III represents sodium bicarbonate waters, and quadrant IV represents calcium sulfate waters.

tion dominance (rainfall), evaporation dominance, and rock-weathering processes. Marandi and Shand (2018) caution that Gibbs diagrams are not always sufficient when interpreting the processes that affect the geochemistry of groundwater. For example, mixing with saline connate groundwater can pull samples to the evaporation influence region of the plot. In our study area there are no ancient marine deposits, so we reject this complication. The Gibbs diagram shows that the low-elevation spring samples which appear to receive some mixture of high-elevation high-salinity recharge fall along a proposed mixing line with this subspace. In addition, Marandi and Shand (2018) specifically state that waters that plot in the upper right corner of the diagram are affected by the presence of surface salts. This is the exact condition which we propose is happening in the connection between saline recharge from the salar and the Chiguata springs. Saline recharge would plot in the evaporative enrichment field where the Laguna Salinas surface waters (LSA) plot. This saline recharge then mixes with fresh groundwater in the mountain block that was recharged by high-elevation snow and/or rain. Thus, Chiguata springs plot between the fields for evaporative enrichment and precipitation dominance. In comparison, springs such as the queñuales forest springs and Pichu Pichu springs, which are supported by high-elevation recharge from snowmelt and/or rain, plot near the precipitation dominance field for anions and rock-weathering for cations. The placement of these endmembers in these fields of the Gibbs diagrams make physical sense. Thus, the Gibbs diagrams appear robust for springs in Characato and Chiguata and for springs and surface waters near Laguna Salinas. The Gibbs diagrams for the major ion compositions of our springs indicate that water chemistry of Characato and Chiguata springs is controlled by water–rock interactions (Fig. 6a and b). Chiguata springs plot at the distal end of the rock dominance region and closer to the evaporation dominance region than the Characato springs. Two springs near Laguna Salinas (UBI and MOQ) also fall in the evaporation dominance area.

High-elevation springs sampled at Pichu Pichu and the queñuales forest area had low  $\text{Cl}^-$  concentrations (Fig. 7). However, high-elevation springs sampled around Laguna Salinas had a wide range of concentrations (Fig. 7a). The Laguna Salinas springs UBI and MOQ had high  $\text{Cl}^-$  concentrations of 2150 and 1400  $\text{mg L}^{-1}$  respectively (Fig. 7a), while springs INK, HUM, TSA, and PAT had  $\text{Cl}^-$  concentrations of 154, 40, 6.5, and 4  $\text{mg L}^{-1}$ , respectively (Fig. 7b). Overall, springs in Chiguata had greater  $\text{Cl}^-$  concentrations than springs in Characato, which are at a lower elevation. This suggests that the springs are not on a single geochemical evolutionary pathway from high elevation to low elevation but are instead supported by groundwater flow paths from different areas of the watershed.

The relationship between  $\text{Cl}^-$  and  $\text{SO}_4^{2-}$  shows two trends: one for Chiguata (BED and BAD) and Characato NaCl (YUM and SAN) springs, with higher  $\text{Cl}^-$  located

along the Río Andamayo fault system, and another one for Characato  $\text{SO}_4^{2-}$  springs, with lower  $\text{Cl}^-$  located in a secondary cluster of shorter faults (Figs. 2 and 8). This relationship between  $\text{Cl}^-$  and  $\text{SO}_4^{2-}$  highlights mixing between recharge from Laguna Salinas (high in  $\text{Cl}^-$  and  $\text{SO}_4^{2-}$ ) and MBR from precipitation occurring on the Pichu Pichu volcano (low in  $\text{Cl}^-$  and  $\text{SO}_4^{2-}$ ). Additionally, the mixing lines (Fig. 8) with two different slopes indicate that Chiguata and Characato NaCl springs have a Laguna Salinas mixing end-member with higher  $\text{Cl}^-$  than the Characato  $\text{SO}_4^{2-}$  springs. The range in  $\text{Cl}^-$  from springs sampled around Lagunas Salinas (Fig. 7b) indicates that there are multiple groundwater flow paths in the high elevations.

## 5 Discussion

Here we discuss evidence of the recharge elevations and groundwater flow paths connecting the Lagunas Salinas salar and the Pichu Pichu volcano to the Chiguata and Characato springs.

### 5.1 Groundwater recharge elevations inferred from stable isotopes

In most orographic precipitation studies along mountain ranges, the stable water isotopic composition of precipitation becomes progressively more depleted at higher elevations (Dansgaard et al., 1964; Clark and Fritz et al., 1997; Rózański et al., 1993). This relationship allows the elevation of spring recharge to be estimated using stable water isotopes. Our observations show that high-elevation snow, springs, and wet-season salar surface waters are isotopically depleted compared to lower elevations (Fig. 3b). However, we observed very little difference in the  $\delta^{18}\text{O}$  and  $\delta^2\text{H}$  between springs at 2533 m in Characato and springs at 3944 m in the queñuales forest, despite the large elevation difference. As observed in Fig. 3a, the springs sampled at the queñuales forest fall very near to the meteoric water line, which suggests that there is no isotopic enrichment of these springs caused by enhanced local evaporation in this ecosystem. Given the nearly identical isotopic values, we believe it is likely that springs in the queñuales forest and Characato share a common recharge elevation of  $\sim 4000$  m or above. We can not conclusively rule out Characato spring recharge by Characato precipitation because the mean 2019 rain isotope value was very similar to the spring values, but the mean 2020 rain isotope values show that many years of observations would be needed to make a meaningful comparison with local rain. The  $^3\text{H}$ -dead waters in Characato also point to high-elevation recharge instead of local. Springs from the Chiguata District have isotopic values that fall between depleted values of Laguna Salinas springs and Pichu Pichu snow and relatively enriched values of the queñuales forest springs (Fig. 3b), which suggests

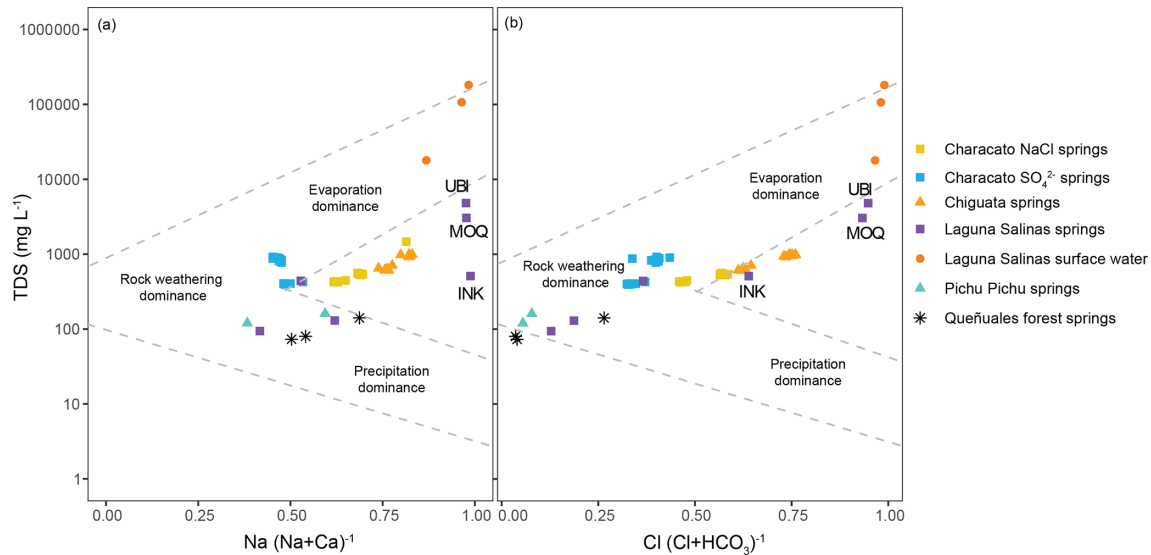


**Figure 6.** Gibbs (a) cation and (b) anion diagram for the ratios of major ion compositions calculated using units of parts per million (ppm). Springs in our study area show a distribution of evaporation, rock weathering, and precipitation influence on the groundwater chemistry. Select springs discussed in the text are labelled with their sample ID.

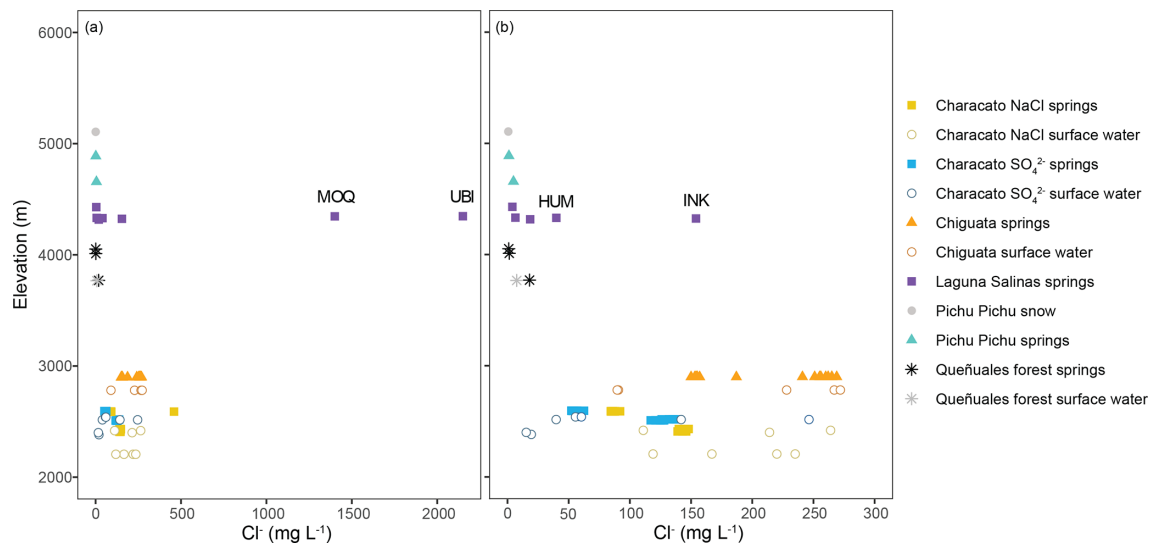


**Figure 7.** Chloride concentration of all water samples at different elevations, (a) excluding Laguna Salinas surface water and (b) excluding two Laguna Salinas springs (UBI and MOQ) with high  $\text{Cl}^-$ .

that Chiguata springs receive a mix of water from higher elevations including possible contributions from snowmelt, medium-elevation queñuales forest springs (presumably fed by rainfall near that elevation), and recharge from the Laguna Salinas in the wet season.

Regionally, the isotopic lapse rate of surface waters in the Western Cordillera is estimated to be  $-10\text{‰}$   $\delta^{18}\text{O}$  per kilometer (Bershaw et al., 2016), which is much larger than observed in this study based on limited precipitation collections ( $\sim -3\text{‰}$   $\delta^{18}\text{O}$  per kilometer from PPI and PRP-Characato data). The factors controlling the isotopic values of precipita-

tion in the Western Cordillera of the Andes are poorly understood, partly due to a lack of data (Valdivielso et al., 2020). Aravena et al. (1999) suggest that the convergence of Pacific and Atlantic moisture sources and the orographic effects of the Western and Coastal Cordilleras could contribute to variability in the lapse rate. Bershaw et al. (2016) values also include evaporation effects of surface waters not included in our approximation.

The springs sampled around Laguna Salinas ( $\sim 4300$  m a.s.l.) have more depleted isotopic values than snow and springs sampled at Pichu Pichu, the local

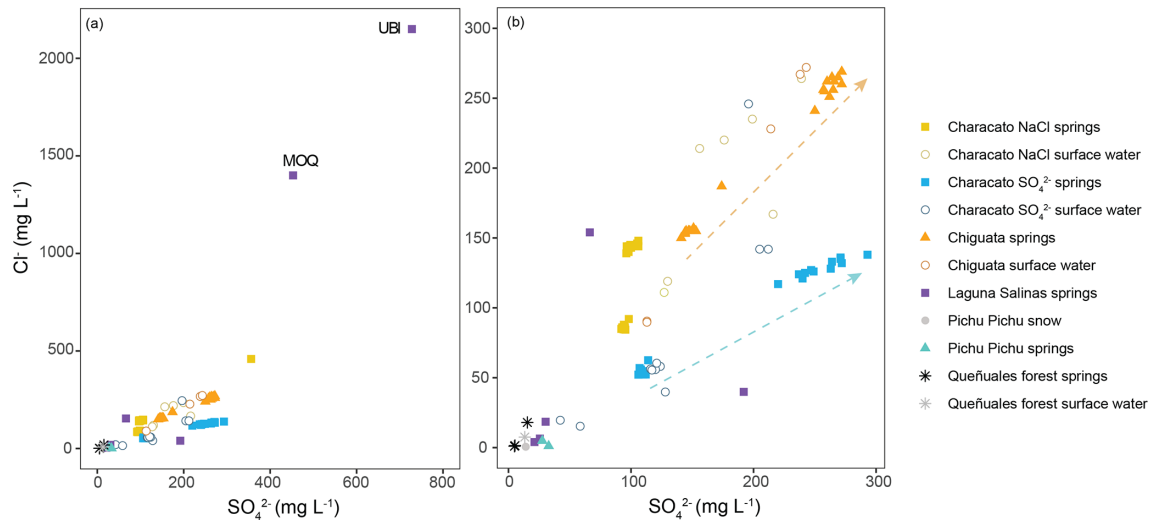


**Figure 8.** Relationships between  $\text{Cl}^-$  and  $\text{SO}_4^{2-}$  of (a) all water samples, except Laguna Salinas surface water, and (b) excluding two Laguna Salinas springs (UBI and MOQ) with high  $\text{Cl}^-$ . Dashed lines indicate patterns of chemical evolution or mixing and not statistical trend lines. The orange evolution line connects springs along the Río Andamayo fault system, and the blue line connects springs in the Characato District furthest from the Río Andamayo in a separate cluster of shorter faults.

peak elevation ( $\sim 5000$  m a.s.l.), and similar to the isotopic composition of Laguna Salinas surface water sampled during the wet season ( $\delta^{18}\text{O} = -16.3\text{‰}$  and  $\delta^2\text{H} = -122.1\text{‰}$ ). This implies that springs around Laguna Salinas are supported by recharge from high-elevation precipitation in region, similar to what flows into the Laguna Salinas basin during the wet season, likely from higher mountain peaks surrounding the salar like the Ubina volcano (5672 m a.s.l.) and Tacune mountains (5500 m a.s.l.). Furthermore, the high-elevation groundwater flow paths are long enough to significantly age the water in springs near the salar (INK and UBI), resulting in non-detectable  $^3\text{H}$  activity.

A subsurface connection between the Ubina volcano, located northeast of the salar, and the Laguna Salinas has been proposed by other studies (Cruz et al., 2019; Gonzales et al., 2014). However, this connection seems unlikely because of vertical rock units along a deep-seated fault to the north-northeast of Laguna Salinas, decreasing the possibility of a hydrogeologic connection to the northeast. It is unclear how far this fault extends to the south. Springs can be seen in Google Earth imagery on the Ubina side of the fault but not toward the Laguna Salinas basin. In any case, if there is a hydrogeologic connection from Ubina to the Laguna Salinas basin, it must occur in a narrow zone immediately east of Ubina. Stable isotope data of a few springs sampled near Ubina volcano and springs at high elevations in the vicinity of Tacune mountain in the adjacent Río Tambo basin show values of  $-15.0\text{‰}$  to  $-16.7\text{‰}$  for  $\delta^{18}\text{O}$  and  $-123\text{‰}$  to  $-130\text{‰}$  for  $\delta^2\text{H}$  (Cruz et al., 2019). While it is plausible that MBR occurring on the slopes of Ubina supports groundwater flow into the Laguna Salinas basin, it is not very probable. However, MBR occurring on Tacune does likely

support groundwater flow into the Laguna Salinas basin; the emergence of high-elevation springs on Tacune cannot be explained otherwise. Another explanation for the depleted isotopic composition of Laguna Salinas springs is paleorecharge from the Last Glacial Maximum (LGM) glacial meltwater stored in the basin. We do not have data to test this conceptual model, but glaciers were present in the vicinity of the Laguna Salinas basin during the LGM (Seltzer, 1990; Juvigné et al., 1997). Additional sampling and dating of springs and wells in the area are necessary to thoroughly test LGM influence.

The long-term stability of the Characato springs' isotopic values within our study period and a sampling from a decade ago indicate that they are supported by a stable source of recharge that is nonresponsive to the temporal short-term variability in rain events within a wet season or interannually. Three of our springs (YUM, OJO, and BED) were also sampled in 2009 by Sulca et al. (2010), and the stable isotopic results obtained in their study were nearly identical to ours 10 years later (Table 2). The  $^3\text{H}$  values of OJO and BED indicate the groundwaters are older than 60 years as well. However, a comparison of spring discharge measurements made once in 1977 and once in 2016 reveals that the discharge from some springs has decreased over this 40-year interval. Spring discharge of Yumina, Ojo de Characato, and La Bedoya was 255, 216, and 206  $\text{L s}^{-1}$ , respectively, in 1977 (Díaz Rodríguez et al., 1978), and 215, 206, and 114  $\text{L s}^{-1}$ , respectively, in 2016 (Peña Laureano, 2018), reflecting decreases of 16 %, 5 %, and 45 % respectively. Differences in discharge may also be due to the variability in time of year the measurements were taken, changes to the La

Bedoya spring channel for water distribution, and possible differences in flow-measurement methodology.

## 5.2 Contribution of groundwater to river flow

While springs showed very little isotopic variability, river isotope data were more variable (Fig. 4). This can be expected for surface runoff since streams and rivers integrate many different flow paths and show an immediate response to precipitation events during the wet season, causing large variations in surface water isotopic values depending on precipitation isotope values. In comparison, the response of springs to precipitation events is slower since groundwater response times are controlled by aquifer diffusivity and are therefore lagged relative to surface-water responses. The upstream reach of the Río Andamayo (ATA) in Chiguata showed a depleted isotopic composition during the wet season (March 2019 and February 2020), which likely indicates the direct runoff input of high-elevation rain. The Río Socabaya (SOC) shows a more depleted isotopic value during February 2020 as the Río Andamayo feeds into the Río Socabaya (Fig. 4). The similarity in isotopic composition between rivers and nearby springs also suggests that the rivers are either being supported by discharge from springs or direct discharge from the same groundwater feeding the springs. This is especially true for the Río Characato (RCH), which shows very little change in its isotopic values (Fig. 4) throughout our sampling period and is extremely similar to its nearest spring, Ojo de Characato (OJO, Table 2).

## 5.3 Insight into groundwater residence times

Two precipitation samples were collected and submitted for  $^3\text{H}$  analyses during this study. The measured  $^3\text{H}$  activity in modern rain from Arequipa (MID) was 1.4 TU, and snow from the Pichu Pichu volcano (PPI) was 2.2 TU. These values are comparable to other modern  $^3\text{H}$  values found in this region of the Central Andes (Aravena et al., 1999; IAEA/WMO, 2012). For example, rainwater collected between 1984 and 1986 in northern Chile was reported to have 3 to 10 TU (Aravena et al., 1999), and precipitation sampled between 2006 and 2012 in Lima, Peru, had  $^3\text{H}$  values that ranged between 2.5 and 5 TU (IAEA, 2012). The atmospheric breakthrough of  $^3\text{H}$  associated with nuclear weapons testing in the 1950s and 1960s for South America peaked at approximately 60 TU in Cuiabá, Brazil, in 1965, while equatorial monitoring stations typically had  $^3\text{H}$  breakthrough activities less than 40 TU (Albero and Panarello, 1981). Although there are latitudinal dependencies in South America similar to those observed in North America, Cuiabá is located close to the same latitude as Arequipa, making it ideal for comparison. In North America, the atmospheric breakthrough of  $^3\text{H}$  was much higher; the tritium breakthrough in Miami, FL, USA, peaked at 384 TU in 1964, while the peak was over 3800 TU in Chicago, IL, USA. In principle,

high-elevation, local-scale groundwater in the mountains surrounding Laguna Salinas should have a  $^3\text{H}$  activity similar to that of high-elevation snow, 2.2 TU. For context, Moran et al. (2019) sampled high-elevation lakes and lagoons that had  $^3\text{H}$  activities of approximately 1.0 TU near the Salar de Atacama in Chile. In comparison, the two high-elevation springs in Laguna Salinas basin (INK and UBI) were  $^3\text{H}$ -dead, indicating long or slow flow paths in local high-elevation recharge and groundwater mixing below the salar. The two lower elevation springs (OJO and BED) were also  $^3\text{H}$ -dead. Relatively old groundwaters are consistent with the nearly constant stable isotope values of the Chiguata and Characato district springs. While it is not possible to provide an accurate residence time based solely on  $^3\text{H}$  data for these springs, we infer that the residence times of springs in the study area are likely greater than 60 years. Ultimately, tritium-dead is ambiguous with respect to residence time; the water sample could be 100 years old, or it could be 100 ka. We cannot confirm or dismiss the possibility of paleo-recharge from the Last Glacial Maximum with only tritium data. Future age dating work should consider using radiocarbon and/or chlorine-36 to provide better constraints on residence times.

## 5.4 Groundwater flow paths

We propose that groundwater mixing within the fractured mountain block controls the  $\text{Cl}^-$  variability in this region. The observed patterns are not consistent with increasing mineral dissolution contributions along increasing flow path length, nor are they invariant due to piston flow through the mountain block (Bresciani et al., 2018, provide a discussion on this topic). Chiguata springs have higher  $\text{Cl}^-$  concentrations even though they emerge at a higher elevation than springs at Characato. Jenks and Goldich (1956) state  $\text{Cl}^-$ -rich groundwater in the region may be explained by weathering of halite crystals found in volcanic deposits, namely a salmon-colored sillar, one of several rhyolitic tuffs present in the Arequipa region. However, the salmon-colored sillar has not been mapped in the Chiguata District to the best of our knowledge. In the absence of salt-bearing minerals, an alternate explanation for this anomaly is that there is a stronger groundwater connection between the high-elevation salar (a source of  $\text{Cl}^-$ -enriched water) and Chiguata springs (Figs. 7 and 8). Both the chemistry and isotopic composition of Chiguata springs point towards a mix of recharge from the Laguna Salinas basin and MBR occurring on Pichu Pichu and potentially other surrounding peaks including Tacune through the salar basin.

We approximated the geochemistry of the groundwater that flows into the Laguna Salinas basin using the chemistry of the INK spring sampled at the salar during the dry season. The validity of using INK as an approximation for groundwater outflow from the Laguna Salinas basin is assessed here by critiquing the chemistry of INK against the geochemical processes responsible for the formation of the evaporite min-

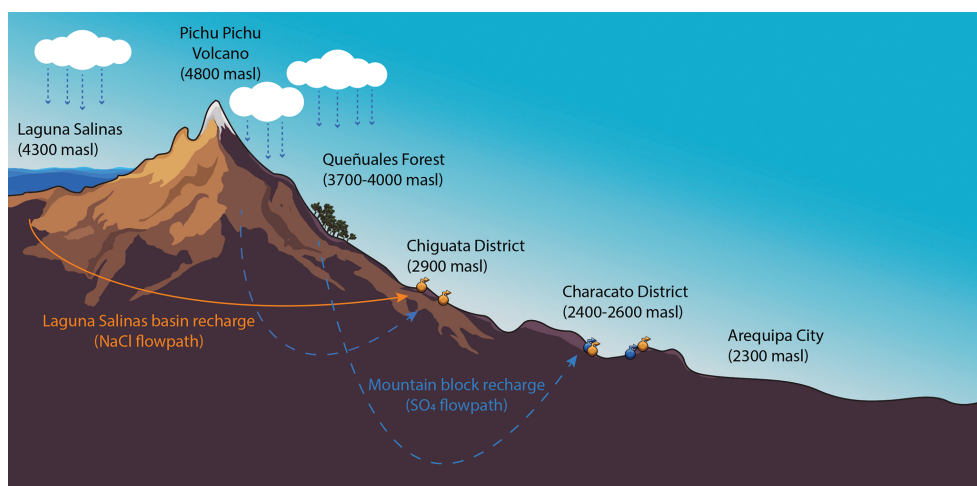


**Figure 9.** Cross section of our study area in the Quilca–Vitor–Chili basin, east of the city of Arequipa. Conceptual model identifying zones of recharge and flow paths in Characato (mountain block recharge (MBR) only) and Chiguata (salar basin recharge and MBR). Note that the conceptual groundwater flow paths do not cross (credit: Diego Alvarez).

erals in the salar. INK is much fresher (510 uScm) than surface salar wet season water (17900 uScm) and Tacune spring water's average (4434 uScm). However freshwater springs (167–181 uScm) from the north and eastern sides of the basin TSA and MNE (Pichu Pichu) could mix with either surface salar or Ubinas waters to create INK waters. INK has high levels ( $2.13 \text{ mg L}^{-1}$ ) of boron (B), which can be explained by B-rich water that enters the salar and subsequent evapoconcentration within the salar during the dry season. Springs HUM and UBI discharging into the basin have high B (greater than  $15 \text{ mg L}^{-1}$  but outside of the analytical calibration used). In any case, the geochemical composition of the spring INK appears to be a mixture of saline waters in contact with evaporites and fresh waters whose geochemical composition can be explained by rock–water interactions (i.e., groundwater flowing from the surrounding mountains and discharging into or around the salar). We observed a high chemical variability in springs surrounding Laguna Salinas that may be influenced by the mineralogy of the Tacune mountain block. Unfortunately, there is little-to-no information on the mineralogy of the rocks of Tacune. We conclude that INK serves as a reasonable approximation of the mixed salar basin groundwater exported via interbasin groundwater flow.

The presence of ulexite nodules in the salar sediments likely points to times of saline water downwelling and fresh water upwelling through the sediments. As stated in Sect. 2.3, the type of evaporite deposits changes with depth in the salar. When the salar begins to evaporate in the dry season, gypsum ( $\text{CaSO}_4 \cdot 2\text{H}_2\text{O}$ ) and anhydrite ( $\text{CaSO}_4$ ) precipitate first, followed by halite (NaCl) and thenardite ( $\text{Na}_2\text{SO}_4$ ) (following the sequence proposed by Garrett, 1998). This increases the concentration of B in the remaining water, some of which likely infiltrates the lacustrine sediments.

The occurrence of ulexite minerals at depths greater than 1.2 m (Garrett, 1998) below the lake surface suggests that the salar level has changed through time, and consequently, the vertical movement of infiltrating water today slows once it reaches the black and green muddy clay layers at 1.2 m. Here, the B-rich water accumulates, and ulexite begins to precipitate (Garrett, 1998; Muessig, 1958). Garrett (1998) states that the most plausible model for the formation of ulexite nodules as opposed to crystal formation requires the mixing of upwelling cation-rich groundwater with downwelling (descending) B-rich water from the surface; the subsequent competition between cation sorption and mineral precipitation in the clay layers favors nodule growth. Since INK discharges into the basin and is flooded during the wet season, this suggests that the salar serves as a local topographic low, which would tend to enhance groundwater discharge or upwelling. Muessig (1958) inferred that the inyoite underlying the ulexite formed in place as a primary mineral from the influx of B-rich water from the nearby hot spring. This specific area of the Laguna Salinas may be similar to the transition zones in the Salar de Atacama described in Boutt et al. (2016), Moran et al. (2019), and Munk et al. (2021). The evaporation rate during the dry season, 141.3 cm (ANA, in 2013), is quite high; however, the influx of surface water to the salar during the wet season is temporarily larger than evaporation rates, causing the salar water level to rise seasonally. Therefore, it is plausible that water can leak from the salar during the wet season.

In immature Andean salars, subsurface sediments are heterogeneous, creating non-isostatic conditions and barriers to flow (McKnight et al., 2021). The heterogeneous nature of these salars facilitates the formation of freshwater lenses that are not dependent on up-gradient flow but rather the result of density-driven flow between surface brines and

freshwater recharged to the salar in the wet season (Munk et al., 2021). Large monsoonal rain events with high rainfall rates have resulted in infiltration of precipitation from the salar surface beneath the transition zone to the underlying halite aquifer in the Salar de Atacama (Boutt et al., 2016). Seepage waters from such events would appear as mixtures of fresh and brine water, so-called transition zone waters (TZWs). We found that shallow inflow waters from Tacune (UBI) and TZWs (INK) were tritium-dead, suggesting long flow paths recharge and mixing occurs beneath the salar. Moran et al. (2019) similarly found that most inflow and TZWs in the Salar de Atacama are tritium-dead, suggesting that these rapid freshwater recharge events observed by Boutt et al. (2016) are a smaller fraction of the overall water budget. If salar seepage does occur during rapid rainfall events, we do not have a representative sample from the local aquifer. Rather, INK is representative of tritium-dead interbasin groundwater flow (IGF) out of the salar basin to Characato and Chiguata springs.

We propose that groundwater recharged on the neighbouring peaks including Pichu Pichu, Tacune, and Pukasaya (the mountains to the north of Lagunas Salinas) and potentially (albeit unlikely) Ubinas flows toward the salar basin, which is a local topographic low. Springs emerge around the basin on the Pichu Pichu, Tacune, and Pukasaya shores of the salar and the spring runs flow into the salar. Subsurface groundwater flow paths also converge on the basin. The groundwater from subsurface flow and from springs mixes with  $\text{Cl}^-$ -rich water that is infiltrating beneath the salar during the wet season. The resulting  $\text{Cl}^-$ -rich groundwater mixture then flows out of the basin, facilitated by extensive faulting in the headwater of the Río Andamayo (Thouret et al., 2001; Bernard et al., 2019; Lebti et al., 2006). The groundwater discharges along a fault at the Chiguata springs. The Río Andamayo is fault-bounded from Laguna Salinas to the city of Arequipa, providing the hydraulic connection between Laguna Salinas and the Chiguata and NaCl Characato springs at lower elevations (Fig. 2).

In comparison, the groundwater which supports the Characato  $\text{SO}_4^{2-}$  springs is geochemically distinct from the Chiguata and Characato NaCl springs (Figs. 5, 6, and 8). The chemical resemblance between Characato springs and high-elevation Pichu Pichu snow and springs (rock weathering dominance in Fig. 6), as well as the isotopic similarities between Characato springs and springs in the mid-elevation queñuales forest (Fig. 3), indicates that the Characato springs are supported primarily by recharge occurring in the mid-elevations to high elevations of Pichu Pichu. The sample of Pichu Pichu snow had  $14.2 \text{ mg L}^{-1}$  of  $\text{SO}_4^{2-}$ , which is higher than expected for typical snow, likely due to aeolian deposition of  $\text{SO}_4^{2-}$  from recent nearby volcanic eruptions like Ubinas. Studies in northern Chile have shown that volcanic eruptions can produce large amounts of air-fall tephra that is deposited in the surrounding mountains and endorheic basins (Warren, 2016). Such events have the potential to ele-

vate sulfate concentrations of waters and snow. We infer that MBR occurring on Pichu Pichu and the queñuales forest zone supports groundwater flow paths on the southwestern slopes of the mountain toward the city as well as flow paths to the northeast into the Laguna Salinas basin. Groundwater flows through distinct sulfate-bearing volcanic deposits toward the Characato District. The Characato springs emerge along several faults on the lower slopes of Pichu Pichu (Fig. 2). It is unlikely that there is significant groundwater circulation on the southwestern slope of Pichu Pichu because this area has been mapped with a landslide deposit overlying a pseudotachylyte (Legros et al., 2000) that probably limits deep circulation.

### 5.5 Conceptual hydrologic models of high-elevation forest and salar connectivity to low-elevation springs

We identify two main recharge zones for the lower elevation Characato and Chiguata springs of our study region based on isotopic and geochemical analyses: (1) MBR within and above the queñuales forest at  $\sim 4000 \text{ m a.s.l.}$  and (2) recharge from the Laguna Salinas basin (Fig. 9). We also identify two main groundwater flow pathways: (1) IGF from the Laguna Salinas basin that provides the characteristic higher  $\text{Cl}^-$  concentration to Chiguata and Characato springs along the Andamayo fault system (Fig. 9), and (2) groundwater flow paths from the Pichu Pichu volcano to lower elevation springs in Characato and Chiguata (Fig. 9).

Our results indicate substantial MBR within or above the queñuales forest; however, forest recharge zones are controversial. Paired forest-logged catchments studies have often found reduced watershed discharge in forested catchments due to higher evapotranspiration rates (see review by Brown et al., 2005). Observations and ecohydrology modelling of the relationship between canopy cover and MBR indicate that snowpack shielding and decreased sublimation may increase recharge in mountain forests (Magruder et al., 2009; Biederman et al., 2015). In general, the relationship between vegetation, water yield, and MBR remains uncertain (Markovich et al., 2019), even as differences in tree types in a single study region have been shown to change water yield (LaMalfa and Ryle, 2008). Therefore, future studies should investigate the ecohydrology of the queñuales forests and their role in MBR.

There have been several proposed hydrological conceptual models for other similar high-elevation closed-basin salars and their influence on lower elevation springs in northern Chile. Some prior studies suggest that there is some degree of hydrogeologic connectivity between high-elevation salars and lower elevation groundwater (Magaritz et al., 1990; Risacher et al., 2003; Herrera et al., 2016; Jayne et al., 2016); however, other studies reject this conceptual model (Uribe et al., 2015; Scheihing et al., 2017, 2018). Our conceptual model conforms with the former, for example, the Herrera et al. (2016) model in the Laguna Tuyajto of northern Chile,

suggesting that closed-basin salars are not simple evaporation pans but instead leakage recharges groundwater flow paths that support lower elevation springs. Our conceptual model is in partial agreement with the findings from local research that identified the zone of groundwater recharge at the Pichu Pichu volcano (Peña, 2018). However, our chemical and isotopic data, as well as inference from fault connectivity, identify the high-elevation Lagunas Salinas closed-basin salar as an additional contributor to groundwater recharge for lower elevations springs and suggest that interbasin groundwater flow is an important hydrogeological process and an influence on the yearlong flow and chemistry of these springs.

Our explanation for the isotopically depleted and Cl- and B-rich source of recharge is that groundwater flow paths originating in the surrounding mountains converge beneath the salar and subsequently flow through fractured volcanic rocks until these flow paths are intercepted by the fault zones along the Río Andamayo. Closed-basin salars like Laguna Salinas often contain thick, clay-rich lacustrine deposits at the bottom of the salar which can impede vertical flow. Very little, if any, recharge must occur in the Laguna Salinas basin during the dry season when evaporation rates are highest or else the isotopic content of the recharge would show the effects of evaporation. Deep groundwater flow paths, in comparison, would preserve the depleted isotopic signal of high-elevation recharge. It seems plausible that the Laguna Salinas basin recharge is a mixture of groundwater flow paths that originate in the surrounding mountains, converge beneath the salar (local topographic low), and mix with wet-season recharge in the salar (leakage from the lake). Ultimately, the isotopic variability of precipitation and the mineralogy of Tacune and the surrounding mountains located north of the salar are poorly quantified. Future studies should (1) investigate the vertical hydraulic conductivity of these lacustrine sediments and quantify their spatial variability in Laguna Salinas, (2) quantify the spatial variability and elevation dependency of precipitation and the stable isotopic composition of precipitation in the mountains surrounding Laguna Salinas, (3) quantify the lithology and mineralogy of the surrounding mountains, and (4) install equipment to close the water balance on the closed basin.

## 6 Conclusions

Our study shows that the Lagunas Salinas basin is not a hydrologic dead end. Instead, it exports a mixture of groundwater from the surrounding mountains and saline water from the salar via interbasin groundwater flow. The salar basin receives groundwater year-round from two primary sources: subsurface flow paths from the surrounding mountains and springs that emerge around the perimeter of the salar and whose spring runs convey water to the salar. However, the salar basin only receives surface runoff during the wet season, causing the water level in the salar to increase. Our con-

ceptual model states that some portion of saline surface water from the Laguna Salinas salar infiltrates the lacustrine sediments during the wet season, mixes with groundwater from the surrounding mountains, and is incorporated into the deeper groundwater flow system. This mixture of water then flows out of the basin by extensive faulting along the Río Andamayo and is brought to the surface in the Chiguata District by faults which crosscut Río Andamayo, where it supports several spring systems. This finding indicates that high-elevation salars may be important sources of recharge supporting low-elevation springs. Recharge area protection is increasingly critical to the sustainability of mountain springs and streams and their associated ecosystems, and our data call attention to careful consideration of connectivity between other high-elevation salars and low-elevation springs in future hydrogeologic studies. Future work should (1) investigate the proposed hydrogeological connection between the salar basin and the Chiguata springs, (2) install wells and instrument the salar basin to better quantify groundwater flow into and out of the salar, and (3) improve the mineral database and expand geologic mapping of the Tacune and Pukasaya mountain blocks. The data presented here provide a framework for protecting the recharge zones surrounding Chiguata and Characato, and the suggested future work would strengthen or refine that framework.

The importance of the queñuales forest, adjacent to Pichu Pichu volcano, for groundwater recharge of low-elevation springs also highlights the need to consider careful management of this natural ecosystem. Water resource planning including that of Chiguata springs, one of which is a main drinking water source to the city of Arequipa (La Bedoya spring), must consider the influence of changes in land use not only at Laguna Salinas where mineral extraction companies currently operate, but also in the mountain block, in and above the queñuales forest. Potential changes in precipitation patterns at the high-elevation closed-basin Laguna Salinas and Pichu Pichu volcano could have impacts on groundwater recharge and long-term maintenance of these lower elevation springs. This study also revealed that there is long-term stability of groundwater in this arid region. Stable isotope measurements of springs and rivers, river discharge, and tritium data support the existence of long flow paths with water residence times of a few decades old or longer. Thus, these data suggest that regional groundwater may provide a stable water resource over the next few decades. While our findings are specific for this region in southern Peru, the implications of climate change, high-elevation forest ecosystem degradation, and influence of the relatively unexplored factor of IGF to low-elevation springs in the Central Andes may translate to other regions of the Andean plateau and Western Cordillera.

Our research informs the origin and flow paths of groundwater resources in this region; however, several questions remain. For instance, what is the percent contribution of each identified recharge zone to spring maintenance, and what is the contribution of rain versus springs to river flow? Water

managers would greatly benefit from learning the answer to these questions to focus their management and conservation efforts of both spring and river waters that are of high importance to socio-economic activities of the region. The combination of isotopic and chemical-based tracers with traditional discharge monitoring, subsurface hydrogeologic mapping, and monitoring of hydraulic head data may be useful techniques to address these questions. However, the use of the latter becomes difficult in remote, poorly accessible areas, such as those found in many areas of our study. Finally, another question that remains is the presence and extent of pre-modern groundwater recharge in this previously glaciated region and the potential influence of paleorecharge to low-elevation spring maintenance, which would have significant implications for sustainable water management in this region. In this arid region of southern Peru, water resources research should continue to investigate the processes that control groundwater and surface water sources and how to best protect and manage them for future use.

**Data availability.** Data used in this analysis are available in the Supplement and are archived in the Purdue University Research Repository (<https://doi.org/10.4231/PJRM-Q992>, Alvarez Campos et al., 2021).

**Supplement.** The supplement related to this article is available online at: <https://doi.org/10.5194/hess-26-483-2022-supplement>.

**Author contributions.** OAC completed data collection, did the laboratory analysis, data analysis, and interpretation and drafted the paper. EJO conducted the data collection, did the laboratory analysis, designed the experiment, interpreted the data, and revised the paper. MDF and LRW led experiment design, interpreted the data, revised the paper, and secured funding for the project. SAZ provided the regional geologic knowledge and participated in the data collection and revision of the paper. JDR provided the regional geologic knowledge and aided in the revision of the paper. WRQ, CSM, and MAC collected the samples, reported the data, and participated in the revision of the paper. The final version of the paper was approved by all authors.

**Competing interests.** The contact author has declared that neither they nor their co-authors have any competing interests

**Disclaimer.** Publisher's note: Copernicus Publications remains neutral with regard to jurisdictional claims in published maps and institutional affiliations.

**Acknowledgements.** The Nexus project director Victor Maque was instrumental in nurturing this international collaboration. We

thank Alexandra L. Meyer and Janine M. Sparks for their assistance in the stable isotope laboratory.

**Financial support.** This work was funded by the Universidad Nacional de San Agustín (UNSA), Peru, through the Arequipa Nexus Institute for Food, Energy, Water, and the Environment.

**Review statement.** This paper was edited by Markus Hrachowitz and reviewed by Ian Cartwright and one anonymous referee.

## References

- Ajami, H., Troch, P. A., Maddock III, T., Meixner, T., and Eastoe, C.: Quantifying mountain block recharge by means of catchment-scale storage-discharge relationships, *Water Resour. Res.*, 47, W04504, <https://doi.org/10.1029/2010WR009598>, 2011.
- Aravena, R., Suzuki, O., Peña, H., Pollastri, A., Fuenzalida, H., and Grilli, A.: Isotopic composition and origin of the precipitation in Northern Chile, *Appl. Geochem.*, 14, 411–422, [https://doi.org/10.1016/S0883-2927\(98\)00067-5](https://doi.org/10.1016/S0883-2927(98)00067-5), 1999.
- Albero, M. C. and Panarello, H. O.: Tritium and stable isotopes in precipitation water in South America, *Interamerican Symposium on Isotope Hydrology*, Bogotá, Colombia, 18–22 August 1981, 91–109, 1981.
- Alvarez Campos, O., Olson, E., Welp, L. R., and Frisbee, M. D.: Groundwater chemistry within Arequipa, Peru in the Characato, Chiguata, and Lagunas Salinas study areas, *Purdue University Research Repository [data set]*, <https://doi.org/10.4231/PJRM-Q992>, 2021.
- Benavente, C., Delgado, G., García, B., Aguirre, E., and Audin, L.: Neotectónica: evolución del relieve y peligro sísmico en la región Arequipa, *INGEMMET, Boletín, Serie C: Geodinámica e Ingeniería Geológica*, 64, 370 pp., 2017.
- Bernard, K., van Wyk de Vries, B., and Thouret, J. C.: Fault textures in volcanic debris-avalanche deposits and transformations into lahars: The Pichu Pichu thrust lobes in south Peru compared to worldwide avalanche deposits, *J. Volcanol. Geoth. Res.*, 371, 116–136, <https://doi.org/10.1016/j.jvolgeores.2019.01.008>, 2019.
- Bershaw, J., Saylor, J. E., Garzzone, C. N., Leier, A., and Sundell, K. E.: Stable isotope variations ( $\delta^{18}\text{O}$  and  $\delta\text{D}$ ) in modern waters across the Andean Plateau, *Geochim. Cosmochim. Ac.*, 194, 310–324, <https://doi.org/10.1016/j.gca.2016.08.011>, 2016.
- Biederman, J., Somor, A., Harpold, A., Gutmann, E., Breshears, D., Troch, P., Gochis, D., Scott, R., Meddens, A., and Brooks, P.: Recent tree die-off has little effect on streamflow in contrast to expected increases from historical studies, *Water Resour. Res.*, 51, 9775–9789, <https://doi.org/10.1002/2015WR017401>, 2015.
- Boutt, D. F., Hynke, S. A., Munk, L. A., and Corenthal, L. G.: Rapid recharge of fresh water to the halite-hosted brine aquifer of Salar de Atacama, Chile, *Hydrol. Process.*, 30, 4720–4740, <https://doi.org/10.1002/hyp.10994>, 2016.
- Bresciani, E., Cranswick, R. H., Banks, E. W., Batlle-Aguilar, J., Cook, P. G., and Batelaan, O.: Using hydraulic head, chloride and electrical conductivity data to distinguish between mountain-

- front and mountain-block recharge to basin aquifers, *Hydrol. Earth Syst. Sci.*, 22, 1629–1648, <https://doi.org/10.5194/hess-22-1629-2018>, 2018.
- Brown, A., Zhang, L., McMahon, T., and Western, A.: A review of paired catchment studies for determining changes in water yield resulting from alterations in vegetation, *J. Hydrol.*, 310, 28–61, <https://doi.org/10.1016/j.jhydrol.2004.12.010>, 2005.
- Camel, V., Quispe-Melgar, H. R., Ames-Martínez, F. N., Navarro Romo, W. C., Segovia-Salcedo, C., and Kessler, M.: Forest structure of three endemic species of the genus *Polylepis* (Rosaceae) in Central Peru, *Ecología Austral*, 29, 285–295, <https://doi.org/10.25260/EA.19.29.3.0.812>, 2019.
- Clark, I. D. and Fritz, P.: *Environmental Isotopes in Hydrogeology*, 1st edn., CRC Press, <https://doi.org/10.1201/9781482242911>, 1997.
- Cruz, V., Pajuelo, D., and Yupa, G.: Caracterización de los sistemas geotermales asociados a los volcanes activos Ubinas y Huaynaputina, región Moquegua, INGEMMET, Boletín, Serie B: Geología Económica, 60, 95–96, 2019.
- Dansgaard, W.: Stable isotopes in precipitation, *Tellus*, 16, 436–468, <https://doi.org/10.3402/tellusa.v16i4.8993>, 1964.
- Díaz Rodríguez, J.: Evaluación Hídrica de la Cuenca de Characato y Alrededores, Ph.D. thesis, Program Académico de Tecnologías Físicas, Geología, Universidad Nacional de San Agustín, Arequipa, Peru, 75 pp., 1978.
- Ehlers, J., Gibbard, P. L., and Hughes, P. D. (Eds.): *Quaternary glaciations—extent and chronology: a closer look*, vol. 15, Elsevier, ISBN 978-0-444-53447-7, 2011.
- Fritz, P., Suzuki, O., Silva, C., and Salati, E.: Isotope hydrology of groundwaters in the Pampa del Tamarugal, Chile, *J. Hydrol.*, 53, 161–184, 1981.
- García Fernández Baca, B., Benavente Escobar, C. L., Delgado Madera, G. F., Aguirre Alegre, E. M., and Albinez Baca, L. A.: Sedimentología y análisis paleosismológico de la cuenca pleistocena Chiguata-Arequipa. XVIII Congreso Peruano de Geología, Arequipa, Peru, 1–4, available at: [http://repositorio.ingemmet.gob.pe/bitstream/20.500.12544/1603/1/Garcia-Sedimentologia...cuenca\\_pleistocena\\_Chiguata.pdf](http://repositorio.ingemmet.gob.pe/bitstream/20.500.12544/1603/1/Garcia-Sedimentologia...cuenca_pleistocena_Chiguata.pdf) (last access: March 2020), 2016.
- Garreaud, R. D.: The Andes climate and weather, *Adv. Geosci.*, 22, 3–11, <https://doi.org/10.5194/adgeo-22-3-2009>, 2009.
- Garrett, D.: *Borates*, Academic Press, 231–234, ISBN 0-12-276060-3, 1998.
- Gerencia Regional de Agricultura de Arequipa: Mejoramiento del servicio de agua para riego en los pueblos tradicionales de Mosopuquio y Cacayaco de los Distritos de Characato y Chiguata, provincia de Arequipa – Región Arequipa, 2015.
- Gonzales, K., Finizola, A., Lénat, J. F., Macedo, O., Ramos, D., Thouret, J. C., Fournier, N., Cruz, V., and Pistre, K.: Asymmetrical structure, hydrothermal system and edifice stability: The case of Ubinas volcano, Peru, revealed by geophysical surveys, *J. Volcanol. Geoth. Res.*, 276, 132–144, <https://doi.org/10.1016/j.jvolgeores.2014.02.020>, 2014.
- Goulden, M. L., Anderson, R. G., Bales, R. C., Kelly, A. E., Meadows, M., and Winston, G. C.: Evapotranspiration along an elevation gradient in California's Sierra Nevada, *J. Geophys. Res.-Biogeosci.*, 117, G03028, <https://doi.org/10.1029/2012JG002027>, 2012.
- Goulden, M. L. and Bales, R. C.: Mountain runoff vulnerability to increased evapotranspiration with vegetation expansion, *P. Natl. Acad. Sci. USA*, 111, 14071–14075, <https://doi.org/10.1073/pnas.1319316111>, 2014.
- Guevara, C.: Geología del cuadrángulo de Characato, INGEMMET, Boletín, Serie A: Carta Geológica Nacional, 23, 1–54, available at: <https://repositorio.ingemmet.gob.pe/handle/20.500.12544/141> (last access: 15 August 2019), 1965.
- Herrera, C., Custodio, E., Chong, G., Lambán, L. J., Riquelme, R., Wilke, H., Jódar, J., Urrutia, J., Urqueta, H., Sarmiento, A., Gamboa, C., and Lictevout, E.: Groundwater flow in a closed basin with a saline shallow lake in a volcanic area: Laguna Tuyajto, northern Chilean Altiplano of the Andes, *Sci. Total Environ.*, 541, 303–318, <https://doi.org/10.1016/j.scitotenv.2015.09.060>, 2016.
- IAEA/WMO: Global Network of Isotopes in Precipitation, The GNIP Database, accessible at: <https://www.iaea.org/services/networks/gnip> (last access: July 2020), 2012.
- Imfeld, N., Sedlmeier, K., Gubler, S., Correa Marrou, K., Davila, C. P., Huerta, A., Lavado-Casimiro, W., Rohrer, M., and Scherrer, S. C.: A combined view on precipitation and temperature climatology and trends in the southern Andes of Peru, *Int. J. Climatol.*, 41, 679–698, <https://doi.org/10.1002/joc.6645>, 2021.
- INEI (Instituto Nacional de Estadística e Informática), Peru: Perfil Sociodemográfico Informe Nacional, Censos Nacionales 2017: XII de Población, VII de Vivienda y III de Comunidades Indígenas, available at: [https://www.inei.gob.pe/media/MenuRecursivo/publicaciones\\_digitales/Est/Lib1539/libro.pdf](https://www.inei.gob.pe/media/MenuRecursivo/publicaciones_digitales/Est/Lib1539/libro.pdf) (last access: 8 December 2019), 2018.
- Jayne, R. S., Pollyea, R. M., Dodd, J. P., Olson, E. J., and Swanson, S. K.: Spatial and temporal constraints on regional-scale groundwater flow in the Pampa del Tamarugal Basin, Atacama Desert, Chile, *Hydrogeol. J.*, 24, 1921–1937, <https://doi.org/10.1007/s10040-016-1454-3>, 2016.
- Jenks, W. F.: Geología del Cuadrángulo de Arequipa, Instituto Geológico del Perú, Boletín No. 9, Lima, available at: <https://repositorio.ingemmet.gob.pe/handle/20.500.12544/2807> (last access: 7 December 2019), 1948.
- Jenks, W. F. and Goldich, S. S.: Rhyolitic tuff flows in southern Peru, *J. Geol.*, 64, 156–172, 1956.
- Juvigné, E., Thouret, J. C., Gilot, E., Gourgaud, A., Graf, K., Leclercq, L., Legros, F., and Uribe, M.: Etude téphrostratigraphique et bioclimatique du Tardiglaciaire et de l'Holocène de la Laguna Salinas, Pérou méridional, *Geogr. Phys. Quatern.*, 51, 219–231, <https://doi.org/10.7202/033120ar>, 1997.
- Kaneoka, I. and Guevara, C.: K–Ar age determinations of late-Tertiary and Quaternary Andean volcanic rocks, southern Peru, *Geochem. J.*, 18, 233–239, <https://doi.org/10.2343/geochemj.18.233>, 1984.
- LaMalfa, E. and Ryle, R.: Differential snowpack accumulation and water dynamics in aspen and conifer communities: Implications for water yield and ecosystem function, *Ecosystems*, 11, 569–581, <https://doi.org/10.1007/s10021-008-9143-2>, 2008.
- Lebti, P. P., Thouret, J. C., Wörner, G., and Fornari, M.: Neogene and Quaternary ignimbrites in the area of Arequipa, Southern Peru: Stratigraphical and petrological correlations, *J. Volcanol. Geoth. Res.*, 154, 251–275, <https://doi.org/10.1016/j.jvolgeores.2006.02.014>, 2006.

- Legros, F.: Minimum volume of a tephra fallout deposit estimated from a single isopach, *J. Volcanol. Geoth. Res.*, 96, 25–32, [https://doi.org/10.1016/S0377-0273\(99\)00135-3](https://doi.org/10.1016/S0377-0273(99)00135-3), 2000.
- Magaritz, M., Aravena, R., Peña, H., Suzuki, O., and Grilli, A.: Water chemistry and isotope study of streams and springs in northern Chile, *J. Hydrol.*, 108, 323–341, [https://doi.org/10.1016/0022-1694\(89\)90292-8](https://doi.org/10.1016/0022-1694(89)90292-8), 1989.
- Magaritz, M., Aravena, R., Peña, H., Suzuki, O., and Grilli, A.: Source of ground water in the deserts of northern Chile: evidence of deep circulation of ground water from the Andes, *Groundwater*, 28, 513–517, <https://doi.org/10.1111/j.1745-6584.1990.tb01706.x>, 1990.
- Magruder, I., Woessner, W., and Running, S.: Ecohydrologic process modeling of mountain block groundwater recharge, *Groundwater*, 47, 774–785, <https://doi.org/10.1111/j.1745-6584.2009.00615.x>, 2009.
- Manning, A. H. and Solomon, D. K.: Using noble gases to investigate mountain-front recharge, *J. Hydrol.*, 275, 194–207, [https://doi.org/10.1016/S0022-1694\(03\)00043-X](https://doi.org/10.1016/S0022-1694(03)00043-X), 2003.
- Marandi, A. and Shand, P.: Groundwater chemistry and the Gibbs diagram, *Appl. Geochem.*, 97, 209–212, <https://doi.org/10.1016/j.apgeochem.2018.07.009>, 2018.
- Markovich, K., Manning, A., Condon, L., and McIntosh, J.: Mountain-block recharge: A review of current understanding, *Water Resour. Res.*, 55, 8278–8304, <https://doi.org/10.1029/2019WR025676>, 2019.
- McKnight, S. V., Boutt, D. F., and Munk, L. A.: Impact of hydrostratigraphic continuity on brine-to-freshwater interface dynamics: Implications from a two-dimensional parametric study in an arid and endorheic basin, *Water Resour. Res.*, 57, e2020WR028302, <https://doi.org/10.1029/2020WR028302>, 2021.
- Ministerio de Comercio Exterior y Turismo (MINCETUR): Reporte Regional de Comercio Arequipa, available at: <https://www.gob.pe/institucion/mincetur/informes-publicaciones/345754-reporte-de-comercio-reporte-comercio-regional-rcr-arequipa-2017-anual> (last access: 7 December 2019), 2017.
- Mering, C., Huaman-Rodrigo, D., Chorowicz, J., Deffontaines, B., and Guillande, R.: New data on the geodynamics of southern Peru from computerized analysis of SPOT and SAR ERS-1 images, *Tectonophysics*, 259, 153–169, [https://doi.org/10.1016/0040-1951\(96\)00034-0](https://doi.org/10.1016/0040-1951(96)00034-0), 1996.
- Minvielle, M. and Garreaud, R. D.: Projecting rainfall changes over the South American Altiplano, *J. Climate*, 24, 4577–4583, <https://doi.org/10.1175/JCLI-D-11-00051.1>, 2011.
- Moraes, A. G., Bowling, L. C., Zeballos Velarde, C. R., and Cherkauer, K. A.: Arequipa Climate Maps – Normals, Purdue University Research Repository [data set], <https://doi.org/10.4231/490D-HC66>, 2019.
- Moran, B. J., Boutt, D. F., and Munk, L. A.: Stable and radioisotope systematics reveal fossil water as fundamental characteristic of arid orogenic-scale groundwater systems, *Water Resour. Res.*, 55, 11295–11315, <https://doi.org/10.1029/2019WR026386>, 2019.
- Muessig, S.: The first known occurrence of inyoite in a playa at Laguna Salinas, Peru, *Am. Mineral.*, 43, 1144–1147, 1958.
- Munk, L. A., Boutt, D. F., Moran, B. J., McKnight, S. V., and Jenckes, J.: Hydrogeologic and geochemical distinctions in freshwater-brine systems of an Andean salar, *Geochem. Geophys. Geosy.*, 22, e2020GC009345, <https://doi.org/10.1029/2020GC009345>, 2021.
- Neukom, R., Rohrer, M., Calanca, P., Salzmann, N., Huggel, C., Acuña, D., Christie, D. A., and Morales, M. S.: Facing unprecedented drying of the Central Andes? Precipitation variability over the period AD 1000–2100, *Environ. Res. Lett.*, 10, 084017, <https://doi.org/10.1088/1748-9326/10/8/084017>, 2015.
- Östlund, H. G., Craig, H., Broecker, W. S., and Spencer, D.: Tritium, in: *GEOSECS Atlantic, Pacific, and Indian Ocean Expeditions, Shorebased Data and Graphics*, Washington DC, National Science Foundation, PANGAEA [data set], 7, 7–10, <https://doi.org/10.1594/PANGAEA.743238>, 1987.
- Peña Laureano, F.: Perímetros de Protección de Manantiales en la Zona Oriental de Arequipa. Informe Técnico No. A6799. Región Arequipa, Instituto Geológico, Minero y Metalúrgico (INGEMMET), available at: <https://repositorio.ingemmet.gob.pe/handle/20.500.12544/1424> (last access: 7 December 2019), 2018.
- Penna, D., Stenni, B., Šanda, M., Wrede, S., Bogaard, T. A., Micheli, M., Fischer, B. M. C., Gobbi, A., Mantese, N., Zuecco, G., Borga, M., Bonazza, M., Sobotková, M., Čejková, B., and Wassenaar, L. I.: Technical Note: Evaluation of between-sample memory effects in the analysis of  $\delta^2\text{H}$  and  $\delta^{18}\text{O}$  of water samples measured by laser spectrometers, *Hydrol. Earth Syst. Sci.*, 16, 3925–3933, <https://doi.org/10.5194/hess-16-3925-2012>, 2012.
- Risacher, F., Hugo, A., and Salazar, C.: The origin of brines and salts in Chilean salars: a hydrochemical review, *Earth-Sci. Rev.*, 63, 249–293, [https://doi.org/10.1016/S0012-8252\(03\)00037-0](https://doi.org/10.1016/S0012-8252(03)00037-0), 2003.
- Rózański, K., Araguás-Araguás, L., and Gonfiantini, R.: Isotopic patterns in modern global precipitation, in: *Continental Isotope Indicators of Climate*, American Geophysical Union Monograph, <https://doi.org/10.1029/GM078p0001>, 1993.
- Scheihing, K. W., Moya, C. E., and Tröger, U.: Insights into Andean slope hydrology: Reservoir characteristics of the thermal Pica spring system, Pampa del Tamarugal, northern Chile, *Hydrogeol. J.*, 25, 1833–1852, <https://doi.org/10.1007/s10040-017-1533-0>, 2017.
- Scheihing, K. W., Moya, C. E., Struck, U., Lictevoud, E., and Tröger, U.: Reassessing hydrological processes that control stable Isotope Tracers in groundwater of the Atacama Desert (Northern Chile), *Hydrology*, 5, 7–11, <https://doi.org/10.3390/hydrology5010003>, 2018.
- Seltzer, G. O.: Recent glacial history and paleoclimate of the Peruvian-Bolivian Andes, *Quaternary Sci. Rev.*, 9, 137–152, [https://doi.org/10.1016/0277-3791\(90\)90015-3](https://doi.org/10.1016/0277-3791(90)90015-3), 1990.
- Sempere, T., Carlier, G., Soler, P., Fornari, M., Carlotto, V., Jacay, J., Arispe, O., Néraudeau, D., Cárdenas, J., Rosas, S., and Jiménez, N.: Late Permian–Middle Jurassic lithospheric thinning in Peru and Bolivia, and its bearing on Andean-age tectonics, *Tectonophysics*, 345, 153–181, [https://doi.org/10.1016/S0040-1951\(01\)00211-6](https://doi.org/10.1016/S0040-1951(01)00211-6), 2002.
- Senamhi: Descarga de Datos Meteorológicos a Nivel Nacional, available at: <https://www.senamhi.gob.pe/?&p=descarga-datos-hidrometeorologicos>, last access: 2020.
- Servicio de Agua Potable y Alcantarillado de Arequipa S. A. (Sedapar): Plan estratégico institucional 2018–2022, Gerencia de Planeamiento y Desarrollo Empresarial, Departamento de Planes y Presupuesto, available at: <https://www.sedapar.com.pe/>

- organizacion/plan-estrategico/ (last access: 7 December 2019), 2018.
- Somers, L. D., McKenzie, J. M., Zipper, S. C., Mark, B. G., Lagos, P., and Baraer, M.: Does hillslope trenching enhance groundwater recharge and baseflow in the Peruvian Andes?, *Hydrol. Process.*, 32, 318–331, <https://doi.org/10.1002/hyp.11423>, 2018.
- Somers, L. D., McKenzie, J. M., Mark, B. G., Lagos, P., Ng, G.-H. C., Wickert, A. D., Yarleque, C., Baraer, M., and Silva, Y.: Groundwater buffers decreasing glacier melt in an Andean watershed – but not forever, *Geophys. Res. Lett.*, 46, 13016–13026, <https://doi.org/10.1029/2019GL084730>, 2019.
- Stensrud, A. B.: Water as Resource and Being: Water Extractivism and Life Projects in Peru, in: *Indigenous Life Projects and Extractivism, Ethnographies of South America*, edited by: Ødegaard, C. V. and Rivera Andía, J. J., Springer, Switzerland, 143–164, <https://doi.org/10.1007/978-3-319-93435-8>, 2019.
- Sulca, P., Peña, F., and Delgado, F.: Determinación de flujos regionales y locales de los acuíferos orientales de la ciudad de Arequipa en base a datos hidroquímicos e isotópicos, XV Congreso Peruano de Geología, Resúmenes Extendidos, Sociedad Geológica del Perú, Pub. Esp. No. 9, Cusco, 128–131, available at: <https://app.ingemmet.gob.pe/biblioteca/pdf/CPG15-032.pdf> (last access: 7 December 2019), 2010.
- Thouret, J. C., Finizola, A., Fornari, M., Legeley-Padovani, A., Suni, J., and Frechen, M.: Geology of El Misti volcano near the city of Arequipa, Peru, *Bull. Geol. Soc. Am.*, 113, 1593–1610, 2001.
- U. S. EPA: Method 200.7: Determination of Metals and Trace Elements in Water and Wastes by Inductively Coupled Plasma-Atomic Emission Spectrometry, Revision 4.4, Cincinnati, OH, 1994.
- U. S. EPA: Method 300.0: Determination of inorganic anions by ion chromatography, Revision 2.1, Cincinnati, OH, 1993.
- Uribe, J., Muñoz, J. F., Gironás, J., Oyarzún, R., Aguirre, E., and Aravena, R.: Assessing groundwater recharge in an Andean closed basin using isotopic characterization and a rainfall-runoff model: Salar del Huasco basin, Chile, *Hydrogeol. J.*, 23, 1535–1551, <https://doi.org/10.1007/s10040-015-1300-z>, 2015.
- Urrutia, R. and Vuille, M.: Climate change projections for the tropical Andes using a regional climate model: Temperature and precipitation simulations for the end of the 21st century, *J. Geophys. Res.*, 114, 1–25, <https://doi.org/10.1029/2008JD011021>, 2009.
- Valdivielso, S., Vázquez-Suñé, E., and Custodio, E.: Origin and variability of oxygen and hydrogen isotopic composition of precipitation in the central Andes: A Review, *J. Hydrol.*, 587, 124899, <https://doi.org/10.1016/j.jhydrol.2020.124899>, 2020.
- Vicente, J. C.: Dynamic paleogeography of the Jurassic Andean Basin: pattern of regression and general considerations on main features, *Revista de la Asociación Geológica Argentina*, 61, 408–437, <https://app.ingemmet.gob.pe/biblioteca/pdf/Paleo-71.pdf> (last access: March 2020), 2006.
- Vuille, M., Carey, M., Huggel, C., Buytaert, W., Rabatel, A., Jacobsen, D., Soruco, A., Villacis, M., Yarleque, C., Timm, O. E., Condom, T., Salzmann, N., and Sicart, J.-E.: Rapid decline of snow and ice in the tropical Andes – Impacts, uncertainties, *Earth-Sci. Rev.*, 176, 195–213, <https://doi.org/10.1016/j.earscirev.2017.09.019>, 2018.
- Wahi, A. K., Hogan, J. F., Ekwurzel, B., Baillie, M. N., and Eastoe, C. J.: Geochemical quantification of semiarid mountain recharge, *Groundwater*, 46, 414–425, <https://doi.org/10.1111/j.1745-6584.2007.00413.x>, 2008.
- Warren, J. K.: Sabkhas, Saline Mudflats and Pans, in: *Evaporites: A Geological Compendium*, 2nd edn., edited by: Warren, J. K., Springer International Publishing, Switzerland, 207–277, <https://doi.org/10.1007/978-3-319-13512-0>, 2016.
- Wilson, J. L. and Guan, H.: Mountain-block hydrology and mountain front recharge, in: *Groundwater recharge in a desert environment: The Southwestern United States*, American Geophysical Union, <https://doi.org/10.1029/009WSA08>, 2004.
- Welp, L. R., Olson, E. J., Valdivia Larrea, A., Reyes Larico, J., Palma Arhuire, E., DeGraw, J., and Michalski, G.: Precipitation isotopes in the Andean Coastal Cordillera reflect the transition between Atlantic and Pacific moisture influence sub-seasonally, in preparation, 2022.